# Electronic structure of copper, silver, and gold impurities in silicon

A. Fazzio,* M. J. Caldas,† and Alex Zunger
*Solar Energy Research Institute, Golden, Colorado 80401*
(Received 11 February 1985)

The electronic structure of Cu, Ag, and Au impurities in silicon is studied self-consistently using the quasiband crystal-field Green's-function method. We find that a substitutional model results in a two-level (acceptor and donor), three-charge-state ($A^+$, $A^0$, and $A^-$) system, which suggests that these defects are amphoteric. Our results show that these substitutional impurities form $e$-type and $t_2$-type crystal-field resonances (CFR) near the center of the valence band and a dangling-bond hybrid (DBH) $t_2$ level in the gap. The $e^{\mathrm{CFR}}$ and $t_2^{\mathrm{CFR}}$ states are fully occupied and represent the perturbed and hybridized impurity atomic orbitals (not simply a "$d^{10}$" configuration). They are magnetically and electrically inactive but are predicted to be optically active in the uv, producing both impurity-bound core excitons as well as localized-to-itinerant $d \rightarrow s$ transitions with their attendant multiplet structure. The $t_2^{\mathrm{DBH}}$ gap level comprises antibonding hybrids of the central impurity orbitals with the vacancy dangling bonds. Its delocalization suggests that both the exchange splitting and the many-electron multiplet separations are small, as opposed to the situation encountered in main-group $3d$ impurities (e.g., Cr, Mn, Fe) in silicon. Consequently, for group-I$B$ impurities, Jahn-Teller distortions should not be suppressed; the magnetic and electrical response of the system is then determined by these split-off components of the $t_2^{\mathrm{DBH}}$ orbital. The calculated donor and acceptor transition energies suggest a 0.15–0.25 eV lattice relaxation energy and that a spin $S=\frac{1}{2}$ resonance may be observed for Si:Au$^0$ if the Fermi energy is located above the donor but below the acceptor energy. Study of the bonding in these systems suggests a depopulation of the atomic $s$ and $d$ orbitals and participation of the metal $p$ orbitals in bond formation. The results of this study conflict both with the Ludwig-Woodbury ionic model and with the $s$ electron (i.e., corelike $d$ orbital) model. Calculations for interstitial gold in Si reveal a hyperdeep $s$-like $a_1$ state just below the valence-band minimum, few $d$-like resonances in the lower part of the valence band, and a virtually bound and delocalized $a_1$ state just near the conduction-band minimum. This state can lead to a simple shallow-donor behavior. Our model for the substitutional and interstitial group-I$B$ impurities is used to discuss site-exchange reactions and to analyze various models employed previously to describe the electronic level schemes for these centers.

## I. INTRODUCTION

The theoretical understanding of transition-atom impurities in semiconductors has progressed remarkably in the last few years.[1–8] Compared with the simpler, $sp$-electron impurities or with isolated lattice defects, the field of $d$-electron impurities in semiconductors exhibits a far richer spectrum of optical, electric, magnetic and structural phenomena (e.g., see the recent review of data in Ref. 9), complementing the well-studied classical fields of $d$-electron impurities in octahedral oxides[10(a)] and coordination chemistry of $d$-electron compounds.[10(b)] Major advances have been achieved through the development of modern, self-consistent computational techniques and systematic studies of *series of impurities* (i.e., rows in the Periodic Table) thereby identifying chemical trends and regularities. The system of group-I$B$ impurities—Cu, Ag, and Au in silicon—although of vast experimental interest,[11–54] has hardly been studied theoretically. In this work we apply the self-consistent quasiband crystal-field Green's-function method to study, for the first time, the chemical trends down a column in the transition series—the $3d$, $4d$, and $5d$ group.

## II. EXPERIMENTAL SITUATION

Group-I$B$ (Cu, Ag, and Au) impurities may be, experimentally, the most studied impurity centers in silicon, judging from the number of publications reviewed recently[11] and from a citation index search. Some of the factors contributing to this proliferation of studies are the common technological use of gold as a minority-carrier lifetime controlling center,[12,13] the role of copper in silicon solar cells,[14] and the technological use of noble-metal contacts to silicon,[15–21] including group-I$B$ silicide formation.[18] We will not try to give a comprehensive review of all data here, but focus instead on the experimentally best-established properties of isolated noble-atom impurities in silicon that are most pertinent to the construction of a model for the electronic structure of these centers. We focus chiefly on the gold center, for which more experimental results are available.

### A. Solubility and diffusion

Group-I$B$ impurities in silicon are superfast interstitial diffusers. Wilcox and LaChapelle[22(a)] have suggested that

 

the diffusion occurs via a substitutional-interstitial vacancy-controlled mechanism. The picture that emerges from their study on Si:Au is one of a rapidly diffusing *interstitial* Au atom (diffusion coefficient at 1200 °C of $D=2.3\times10^{-5}$ cm$^2$/sec) capturing the mobile[55] vacancies to form *substitutional* gold, which is essentially immobile (diffusion coefficient at 1200 °C of $D=2.9\times10^{-10}$ cm$^2$/sec). An alternative "kick-out" mechanism,[22(b)] in which an interstitial impurity kicks a substitutional host silicon atom off its site, producing interstitial silicon and a substitutional impurity, seems very plausible too. When a high-vacancy concentration is available (e.g., Ge), the vacancy-diffusion mechanism may dominate over the kick-out mechanism. The diffusion activation barriers were determined to be $8.9\pm2$ kcal/mole for the interstitial mechanism and a much larger value of $47\pm10$ kcal/mole for the substitutional mechanism. This suggests that most of the gold would eventually be trapped in substitutional sites. The fast interstitial diffusion suggests that the final geometry of the substitutionally trapped impurity will depend on the details (i.e., temperature rate) of the quenching and annealing.[22(c)] Indeed, Morooka *et al.*[22(c)] observed a high-temperature undistorted substitutional Au in Si as well as a low-temperature (conventional) off-substitutional gold. Analysis of the system's enthropy led Van Vechten and Thurmond[24] to conclude that the gold center was probably coupled to a lattice vacancy remaining in some off-substitutional site. The interstitial ($i$) solubility $S_i(T)$ was determined[22,23] to be

$$S_i(T)=5.95\times10^{24}\exp[(-58\pm10\text{ kcal})/RT]\ ,$$

whereas the substitutional(s) solubility was

$$S_s(T)=8.15\times10^{22}\exp[(-40.6\text{ kcal})/RT]\ ,$$

both below 1200 °C. For Si:Cu, the interstitial diffusion coefficient is $0.76\times10^{-5}$ cm$^2$/sec at 500 °C (it is the fastest interstitial-diffusing species in silicon) with an activation energy of 9.9 kcal/mole. A similarly large diffusion coefficient was observed[26] for silver in silicon. A survey of solubility data[27] indicates that group-I*B* impurities have among the largest solubilities of all transition atoms in silicon, with a maximum of $\sim10^{17}$ cm$^{-3}$ and $10^{18}$ cm$^{-3}$ for Au and Cu, respectively, around 1300 °C. Interestingly, the substitutional-to-interstitial solubility ratio is found to depend strongly on both the impurity[25(a),25(b)] (i.e., Cu, Ag, or Au) and the host crystal,[25(a)] (Si or Ge) but a clear doping-induced solubility enhancement is observed for a fixed impurity-host pair. Electrolysis experiments[23] show that Cu diffusion in Si at 1100 °C is field dependent (whereas that of Au is not) suggesting that Cu diffuses as a charged $Cu^+$ species. The relatively large solubility and superfast interstitial diffusion have significant implications on both the electric properties and the chemical characteristics of group-I*B* impurities. We review these next.

### B. Complexes

The large diffusion constants of group-I*B* interstitial impurities suggest that even under rapid quenching conditions it is difficult to initially trap those impurities in substitutional sites. This, together with the large electronegativity of gold (2.4 on Pauling's scale), contributes to the formation of numerous complexes, both with intentionally introduced electropositive dopants and unintentional trace impurities. Among these we note the iron-gold complexes[13] observed[29] in electron paramagnetic resonance (EPR), the oxygen-gold complex,[12] the phosphorus-gold complex,[25(b),30] numerous complexes between $3d$ impurities and gold,[31] and between copper and various donors.[25(a)] The occurrence of these (often) uncontrolled material- and processing-dependent complexes is a major factor contributing both to the poor reproducibility of many experimental results and to the slow progress made over the past 30 years in developing a comprehensive, microscopic model for the *isolated* group-I*B* centers. Note, however, that despite the ample evidence for complexes of Au in Si, it does not follow that they are related to the acceptor and donor levels usually attributed to isolated Au. Even if completely different defect centers might accidentally show similar ionization energies,[40] one would expect that coupling of the same impurity (Au) with such different partners as iron or oxygen would produce substantial shifts in the ionization energies of the center (at least if the impurity pair were brought close together, e.g., to nearest-neighbor distance). Even if the complex defect were thought of as a pair of impurities interacting via charge transfer through a distance of a few bond lengths,[29] the isolated impurity model might still be valid for most practical purposes.

### C. Electrical levels

The inability to quench sufficiently rapidly copper impurities in silicon (they precipitate as clusters[32] or oxygen complexes[12,14]) leads to the appearance of a multitude of copper-related species and a corresponding spread in electrical levels, essentially covering the entire band gap of silicon.[32] It appears that experiment alone could not determine the electrical levels of an isolated Cu impurity in silicon, although substantial evidence points to its being a triple acceptor with no donor action.[25(a)] The situation is somewhat clearer for Si:Ag and Si:Au. For Si:Ag, many workers argue (e.g., Refs. 33 and 35) that it is associated with an acceptor level at $E(0/-)\simeq E_c-0.29$ eV and a donor level at $E(0/+)\simeq E_v+0.32\pm0.05$ eV, but Yau and Sah[41(b)] suggest those to be at $E(0/-)=E_c-0.593$ eV and $E(0/+)=E_v+0.405$ eV, respectively, and Fahrner and Goetzberger[43] find $E(0/-)=E_c-0.36$ eV and $E(0/+)=E_v+0.33$ eV. In recent works,[36] Tavendale and Pearton have reported for Si:Ag a hole trap at $E_v+0.48$ eV, and determined that the donor state occurs at $E_v+0.29$ eV in $p$-type Si, and that the acceptor state occurs at $E_c-0.54$ eV in $n$-type Si (a value which agrees more closely with the results of Yau and Sah[41(b)]). For Si:Au, the best-established results[32–44] show the occurrence of an acceptor in $n$-type Si at $E(0/-)=E_v+0.63$ eV and a donor at $E(0/+)=E_v+0.35$ eV in $p$-type Si. These values have been determined by means of a direct acceptor electron-trapping technique,[32] junction photocurrent measurements,[38] direct photoconductivity,[44] or deep-level transient spectroscopy[41–43] (DLTS),

and they include the standard $T^2$ temperature correction. The overall picture is that Si:Cu has a triple acceptor (indicating that it takes a substitutional or near-substitutional site), but Si:Ag and Si:Au have a single acceptor and a single donor each.

In the work of Braun and Grimmeiss,[38] threshold energies were measured for the Au acceptor, both through electron emission from the conduction band (at $E_c-0.555$ eV) and through hole emission from the valence band (at $E_v+0.61$ eV). The sum of these energies (1.166 eV) was close to the Si band gap at the temperature at which the experiment was done, suggesting that the gap level relaxes in a similar way when the carrier is either in the conduction or the valence band. For the Au donor, the corresponding results were $E_c-(0.75-0.83)$ eV for electron emission and $E_v+0.345$ for hole emission, which similarly implies a small net relaxation difference. Photoluminescence experiments[45] show a sharp emission line and a peak at 0.78 eV (i.e., at $\sim E_v+0.37$ eV), which is attributed to the donor final state. This is close to the value of $\sim E_v+0.345$ eV obtained under equilibrium thermal emission.

Using the best-established values for the single-acceptor and single-donor energies of Si:Au, one would obtain an effective Mott-Hubbard Coulomb repulsion energy of $U\equiv E(0/+)-E(0/-)\simeq 0.28$ eV, if it were assumed that both transitions resulted from the same center (i.e., the impurity was "amphoteric"). For Si:Ag, one obtains $U=0.32$ eV. This point is, however, the subject of an ongoing controversy. We discuss this point next.

### D. Is Si:Au amphoteric?

Whereas twenty years ago it seemed to have been universally accepted that gold forms a substitutional impurity in silicon, and that this center is responsible both for the acceptor level at $E(0/-)=E_v+0.63$ eV and the donor level $E(0/+)=E_v+0.35$ eV (amphoteric center), recent conflicting measurements on emission and capture cross sections have raised some doubts on this identification. A recent compilation[11] of cross sections for these transitions shows a bewildering spread of data obtained by modern techniques on high-purity silicon in different laboratories. Lang *et al.*[40] have conducted a series of measurements on diodes made from Czochralski-type Si and from epitaxially-grown Si and found sufficiently different characteristics of the acceptor emission data in both cases to conclude that there is no single Au-related acceptor state in Si. Paradoxically, however, comparison of the acceptor thermal emission rates of Si:Au to five other midgap levels (Ag, Co, Rh, S, and process-induced levels) showed all to be identical. The apparently different concentration of the donor and acceptor electrical levels[40] in Si:Au (although most differences were within experimental uncertainties) had further supported the contention of Lang *et al.* that these levels do not belong to the same center. Similarly, Wu and Peaker[13] have observed, in support of this suggestion, that differences in emission cross sections correspond approximately to different impurity diffusion treatments. However, they did not rule out the possibility of Au being amphoteric (different material treatments alter the impurity distribution, electric and strain fields).[22(c)]

These controversies have motivated Ledebo and Wang[46] to undertake a careful measurement of the time dependence of the occupation numbers for the donor and acceptor states in Si:Au during optical excitations. Their data give strong evidence that *both levels correspond to the same single defect, i.e., that Si:Au is an amphoteric center.* The conclusion that Si:Au is a two-level (donor and acceptor), three-charge-state ($Au^+$, $Au^0$, and $Au^-$) system has been further corroborated by the analysis of profile concentrations of both levels by capacitance transients and by Au-Fe pairing[30] (in particular, the observation of the reappearance of isolated gold signals after thermal dissociation of the Au-Fe complex[30(b)]). Furthermore, it has been recently suggested[47] that apparent differences in concentrations of the acceptor and donor levels[40] are consistent with an amphoteric center, based on the occurrence of electron-hole exchange transitions. (This suggestion, however, may not even be needed to explain the data.[46])

### E. Degeneracy factor

The temperature dependence of emission rates involves both the exponential factor of the transition enthalpy and a preexponential factor $X_i=\exp(\Delta S_i/k)$ related to the transition entropy $\Delta S_i$ for $i=p$ or $n$, corresponding to $p$- and $n$-type doping, respectively.[40,49(a)] The entropy change includes both electronic and vibrational (vib in superscript) components, the former being simply the ratio $g_0/g_1$ of the level degeneracy of the empty level ($g_0$) and the singly occupied electronic level ($g_1$). Hence, the degeneracy factors are $X_n=g_0/g_1\exp(\Delta S_n^{\rm vib}/k)$ for $n$-type materials and $X_p=g_1/g_0\exp(\Delta S_p^{\rm vib}/k)$ for $p$-type materials, where $\Delta S_i^{\rm vib}$ are the corresponding vibrational transition entropies. Thus, measurement of the temperature dependence of the emission rates can be used to deduce the electron level degeneracies $g_\alpha$ and aid in the identification of the emitting level. Such experimental studies have produced widely conflicting results: e.g., $X_n=48$ and 20, both obtained by Lang *et al.*[40] from their two samples: $X_n=47.5$, obtained by the same authors from the data of Brotherton and Bicknell,[37] and $X_n=1.04$, from the data of Nagasawa and Schulz.[48] Brotherton and Lowther[49(b)] have obtained $X_n=38$ and have noted that a similar calculation of $X_n$ for the Pt acceptor ($Pt^-$ is isoelectronic with $Au^0$) yields a far smaller value of $X_n$ (0.5), which suggested to them that the acceptor transition in Si:Au involves a far larger entropy (i.e., lattice distortions) change than that in Si:$Pt^-$. From their estimate of the vibrational entropy $\Delta S_n^{\rm vib}=2.85k$ (based on equating it with the corresponding change in the band-gap entropy) they deduce $g_0/g_1=X_n\exp(-2.85)=2.2$, using their value $X_n=38$ for the Si:Au acceptor. Assuming zero vibrational entropy change for the corresponding transition in Pt, they obtain $g_0/g_1=X_n\simeq 0.5$ for Si:$Pt^-$. The different electronic degeneracy factors for Si:Au and Si:$Pt^-$ were interpreted by Brotherton and Lowther[49] to suggest that the acceptor transitions in Au and Pt commenced from different one-electron levels. This conclusion appears, however, to be questionable in view of the large

scatter in temperature dependence of the emission rates and the corresponding scatter in the $X_n$ values for Si:Au ($1 \leq X_n \leq 48$).

Fewer experimental values are available for the donor degeneracy factor $X_p$. Lang *et al.*[40] found $X_p = 5.7$, whereas Brotherton and Lowther[49(b)] suggested from their data that $X_p = 3.6$. This is similar to $X_p = 3.7$, which they deduced for the Pt center, suggesting to them a similar transition in both cases, one related primarily to an impurity *s*-like level rather than a lattice-vacancy-like level. However, a recent very careful study[50] showed $X_p = 20$, close to the value $X_p = 16$ obtained earlier by Brückner.[51] Accepting this recent value $X_p = 20 \pm 2$, obtained by two independent methods with two different devices on the same Si wafer, one concludes that Lowther's conclusion of the similar origin of the donor transitions in Si:Au and Si:$Pt^-$ and his contention that acceptor and donor transitions in Si:Au commence from two different levels (with large and small relaxation changes, respectively) are both unsupported by recent data.

The way in which degeneracy factors can be used to delineate different electronic structure models for these centers has been illustrated by Ralph.[52] He considered two possible energy-level models for Si:Au: the one-electron level, leading to acceptor and donor action, could be either ligandlike (i.e., *p*-type orbitals) or impuritylike (i.e., *d*-type orbitals). In the first case, the neutral and negatively charged centers $Au^0$ and $Au^-$ would have $p^3$ and $p^4$ configurations, respectively; whereas, in the latter case, the configurations would be $d^7$ and $d^8$, respectively. These differing possibilities would then lead to different predictions of electronic degeneracies. Ralph then obtained the many-electron multiplet terms appropriate for either case and delineated the ground-state from the excited-state configurations on the basis of an assumption of strong Coulomb and spin-orbit interactions. Hence, he obtained (acceptor) electronic degeneracy factors ranging from $\frac{2}{3}$ to 4 for the *p*-orbital model and a degeneracy factor of 4 for the *d*-orbital model. Although the results were not conclusive and omitted the vibrational entropy factor, he favored the latter results on the assumption that the electrically active levels in Si:Au were presumably similar to those in 3*d*-doped Si, where the overriding role of the *d* component had been established. This question of the orbital origin of the electrically active gap levels remained unsolved.

### F. Electron paramagnetic resonance

Another factor contributing to the lack of a microscopic model for group-I*B* impurities in Si is the failure to observe any EPR that could be associated with an isolated impurity. Recently, Höhne[53] observed the EPR of gold-related centers in Si. In addition to the signal of Cu-Au clusters, he also observed another center with a highly anisotropic *g* factor, suggestive of a very low $C_{1h}$ symmetry. He concluded that since a Jahn-Teller (JT) distortion cannot lower the symmetry below $C_{2v}$, the even lower $C_{1h}$ symmetry he observed had to be related to complex formation with a nearby defect, such as carbon, sulfur, or a 3*d* atom. Two other centers [denoted[53] as Au(1) and Au(2)] were initially thought to be related to substitutional gold; however, Kleinhenz and co-workers[29(a),29(b)] showed that the Au(1) spectrum was identical to that of the Fe-Au complex observed by them earlier.[29(a)] The failure to observe an isolated Au EPR signal even at a He temperature[54] is surprising, since the isoelectronic $Pt^-$ center has long been known to produce a distinctive signal,[56,57] displaying a dihedral distortion associated presumably with a tetragonal deformation, with a possible small trigonal component and a spin $S = \frac{1}{2}$. The fact that $Pt^-$ gives such a spin value itself is surprising,[56] since a standard ionic model (cf. Sec. III A) would predict that the $d^9s^2$ state of the isolated $Pt^-$ ion would become $d^7$ when $Pt^-$ replaced the tetravalent silicon atom to form a substitutional impurity. Such $d^7$ configurations in tetrahedral substitutional symmetry are known[56] to give three unpaired electrons with spin $S = \frac{3}{2}$. Recent suggestions[57(a)] that the observed $Pt^-$ center involves Pt-Pt pairs have been disputed.[57(b)]

Symmetry information, usually found through EPR experiments, can also be deduced from the study of optical transitions and ion backscattering. Thebault *et al.*[58] studied the 0.78-eV luminescence band of the gold center at high resolution and concluded that the zero-phonon luminescence originated from an internal transition at the Au defect. From the line structure, the authors deduced that the symmetry of the center was lowered from $T_d$, although they could not give a detailed model for the distortion. Ion backscattering experiments[25(b)] on Si:Au suggest that almost all of the gold is on the substitutional site; however, within the precision of the data and its analysis it is not possible to distinguish the exact substitutional site from a slightly distorted substitutional site.

### G. Photoemission

It is not common to apply photoemission techniques to study impurities in semiconductors, since their solubility limit is often below that necessary to observe photoemission. However, contacts of gold and silver to silicon are known to produce,[15–21] past a critical layer thickness and deposition temperature, an intermixed layer characteristic of dilute noble-metal silicides, with large metal-metal distances, well above the bulk metallic values. While the concentrations often exceed the impurity equilibrium solubility limit, chemical shifts in the metal *d* states due to concentration changes[15–21] do not exceed $\sim 1$ eV. Within this range, it is possible to determine from such studies the approximate energy location of the occupied group-I*B*—induced levels *inside the valence band,* information that cannot be obtained from electrical measurements. Such experiments indicate that under conditions where the noble-metal atoms are dispersed inside silicon in a dilute form, one observes both a noble-metal *d* signal and changes in the *s*-electron density of states at the lower part of the valence band. For instance, Au in Si produces a 5*d* spin-orbit doublet around[19] $\sim E_v - 6$ eV. This Au 5*d* structure moves to somewhat higher binding energies as the temperature is raised, and a better sample homogenization is obtained. This structure arises unambiguously from Au (as characteristic gold core levels are simultane-

ously observed) and was interpreted[19,21] as arising from bonding combinations of Au $5d$ with Si $sp^3$ orbitals. In addition to this structure, another signal appears[15] at higher binding energies, around $E_v-10\pm1$ eV, because of modification (rehybridization) in the $s$-orbital density of states. For the Si:Ag system,[20,21] the Ag $4d$-induced state appears around $E_v-4.3$ eV, and the $s$-like state appears around $E_v-11$ eV. These studies indicate unequivocally that the noble-metal $d$ electrons cannot be considered as chemically inert, since their levels appear in the upper part of the valence band, much as in noble-atom intermetallic compounds, or chalcopyrites (e.g., $CuGaS_2$), or group-I$B$ halides.

### H. Summary

From the survey of the observed properties of group-I$B$ impurities in silicon, we find the following points to be both significant and interesting.

(i) Interstitial diffusivity is very high; substitutional diffusivity is extremely low. An intriguing free-carrier dependence of the solubility is present.

(ii) Chemical complexes and precipitates overshadow many of the properties of the isolated impurities and imply that extra caution (and skepticism) has to be exercised in interpreting the data in terms of isolated impurities.

(iii) These impurities are most probably amphoteric and consistently show for Si:Au a single acceptor level at $\sim E_v+0.63$ eV in $n$-type material and a single donor level at $\sim E_v+0.35$ eV in $p$-type material, whereas the corresponding values for Si:Ag are an acceptor around $E_v+0.6$ eV and a donor around $E_v+0.3$ eV. No such levels could be determined with any certainty for Si:Cu. If one assumes the gold center to be amphoteric, the data imply an effective electron-electron repulsion of $U(\mathrm{Au}^0)\simeq0.28$ eV and $U(\mathrm{Ag}^0)\simeq0.3$ eV, characteristic both of the Si unrelaxed vacancy and other $3d$ impurities in Si (e.g., Fe, Mn, Cr).

(iv) No reliable information can yet be extracted from the measured degeneracy factors, although the data seem to point to a substantial relaxation entropy for both acceptor and donor transitions in Si:Au. Analysis of the data does not point conclusively to either ligandlike ($p$-orbital) or metallike ($d$-orbital) characteristics of the gap levels.

(v) Surprisingly, no EPR signal was observed for $\mathrm{Si:Au}^0$, although its isovalent impurity $\mathrm{Si:Pt}^-$ shows a $S=\frac{1}{2}$ spectra with substantial atom pairing consistent with a tetragonal distortion (with a possible small trigonal component) reminiscent of that of the negatively charged silicon vacancy $V^-$.

(vi) Photoemission data show that the noble-metal $d$ electrons show up as a resonance in the upper part of the Si valence band (in the range of $E_v-4$ to $E_v-6$ eV) and hence cannot be considered chemically inert. In addition, an $s$-electron structure appears in the lower part of the valence band around $E_v-(10\pm1)$ eV.

One cannot avoid the conclusion that the present understanding of the nature of the states of noble-atom impurities in silicon, after 30 years of intense experimental studies, is at best sketchy. Therefore, we review next the *conceptual models* that have been previously adapted to similar systems, in an attempt to establish the basic physical features and open theoretical issues of this system.

## III. CONCEPTUAL MODELS

### A. Ionic model

The most successful model for describing qualitatively the electronic structure of $d$-electron substitutional impurities in silicon is that of Ludwig and Woodbury[59] (LW), a model that has also been applied since its description over 20 years ago of $3d$-electron impurities in many other semiconductors.[60]

The model assumes that the fivefold degenerate atomic $d$ orbital (tenfold, including spin) is split in the substitutional tetrahedral site symmetry of the solid into a twofold degenerate $e$ orbital (fourfold, including spin) and a threefold degenerate $t_2$ orbital (sixfold, including spin) located at higher energy by the amount $\Delta_{\mathrm{CF}}$ ("crystal-field splitting," CF). Out of the $N$ valence electrons of the free atom in the configuration $d^n s^m$ (with $N=n+m$), a number $M$ equal to the valence of the host atom being replaced ($M=4$ in Si, $M=3$ in $Ga$As, and $M=2$ in $Mg$O) are supplied to remake the broken bonds, leaving $n+m-M$ electrons to occupy the $e$ and $t_2$ "gap levels," associated with the metal $d$ states. This assumption implies that, in the neutral state of the impurity, $M$ fewer electrons are available to it relative to the free atom. Hence, its oxidation state becomes $+M$; e.g., Cu(1) for neutral $Na$Cl:$\mathrm{Cu}^0$, Fe(2) for $Mg$O:$\mathrm{Fe}^0$, and Cr(3) for $Ga$As:$\mathrm{Cr}^0$. These missing electrons are said to be taken first from the metal $s$ orbital, i.e., an $s\rightarrow d$ population inversion is said to occur. LW assumed, from the abundant data on $d$-electron impurities in oxides available at the time (e.g., reviews in Refs. 61 and 62), that these $n+m-M$ electrons occupied the gap levels in such a way that the maximum spin $S$ was attained (Hund's rule). For example, for Mn, Fe, and Co with $N=7$, 8, and 9 electrons, respectively, the configurations of the neutral centers in silicon ($M=4$) were $e^2t_2^1$, $e^2t_2^2$, and $e^2t_2^3$, respectively, and the oxidation state was $4+$ for all neutral centers. These configurations would have violated the Fermi statistics (holes are left in the $e$ orbital below the occupied $t_2$ orbital), were it not for the additional assumption that each of these space orbitals is further split by the exchange ($x$) interaction $\Delta_x$ into spin-up ($t_+$ and $e_+$) and spin-down ($t_-$ and $e_-$) components, and that the level ordering is $e_+<t_+<e_-<t_-$, i.e., the $t_+$ level crosses the $e_-$ level, or $\Delta_x>\Delta_{\mathrm{CF}}$. This leads to the configurations $e_+^2t_+^1e_-^0t_-^0$, $e_+^2t_+^2e_-^0t_-^0$, and $e_+^2t_+^3e_-^0t_-^0$ for neutral substitutional Mn, Fe, and Co impurities, respectively, in silicon, i.e., the *aufbau* principle of successive shell filling is fulfilled. We refer to this level ordering as "high-spin-like" (HSL), to distinguish it from the "low-spin-like" (LSL) ordering of $e_+<e_-<t_+<t_-$, where the $t_+$ level does not cross below the $e_-$ level. The single assumption of a HSL-level ordering for all $d$ impurities was sufficient in the LW model to explain the spin values and the trends in $g$ values (including temperature effects) in a number of $d$-electron impurities in Si which were known at that time. The same model was extended with similar success[60] to all $3d$ impurities in GaAs, GaP, and InP.

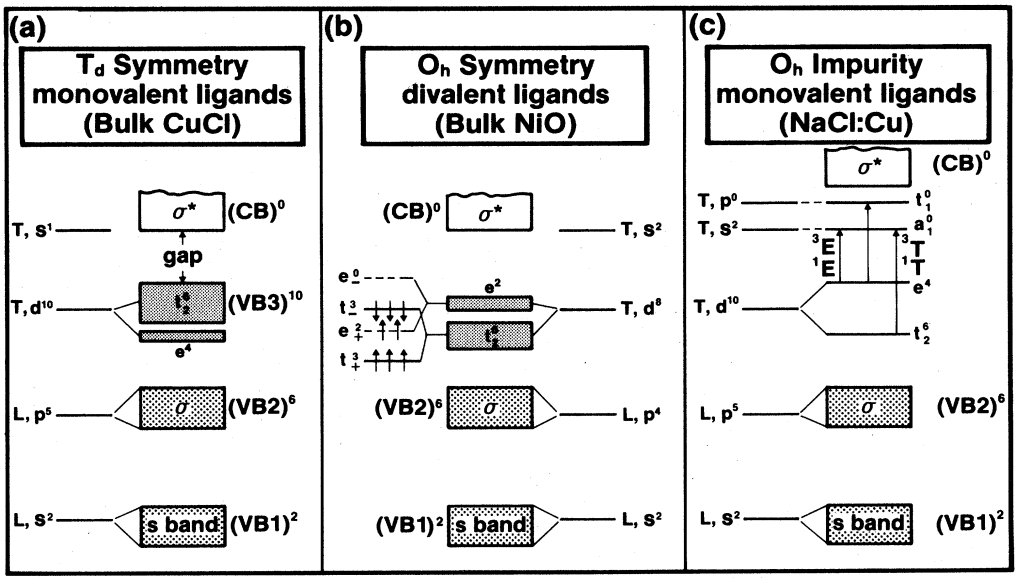


FIG. 1. Application of the ionic model to deduce the energy-level structure of (a) bulk CuCl, (b) bulk NiO, and (c) NaCl:Cu. $L$ denotes ligand orbitals, $T$ denotes transition-atom orbitals.

The LW model is essentially identical to similar models used at the time of their work to explain the properties of $d$-electron impurities in ionic cubic oxides (e.g., review articles in Refs. 61 and 62) or the band structure of bulk transition-metal oxides (e.g., reviews in Refs. 63 and 64). The only significant difference is that in the tetrahedral-site symmetry of Si, the $e$ level is below the $t_2$ level, whereas in octahedrally coordinated (i.e., $O_h$) oxides (e.g., MgO, NiO) the order is reversed. The application of the model to bulk compounds is illustrated in Fig. 1. Using first the tetrahedrally coordinated CuCl as an example [Fig. 1(a)], the chlorine $p$ orbital, having five electrons in the neutral atomic state, is assumed to lie lower in energy than the metal $d$ orbitals, occupied by ten electrons. As metal-ligand bonding is switched on, the chlorine $p$ band becomes fully occupied by removing the $M=1$ electron from atomic Cu $d^{10}s^1$. It forms the occupied Cl $p$ band (VB2), above the Cl $s$ band (VB1). The $n+m-M=10$ electrons left on $Cu^+$ fill the metal $e$ and $t_2$ orbitals in a closed-shell $e^4t_2^6$ configuration which forms in CuCl the

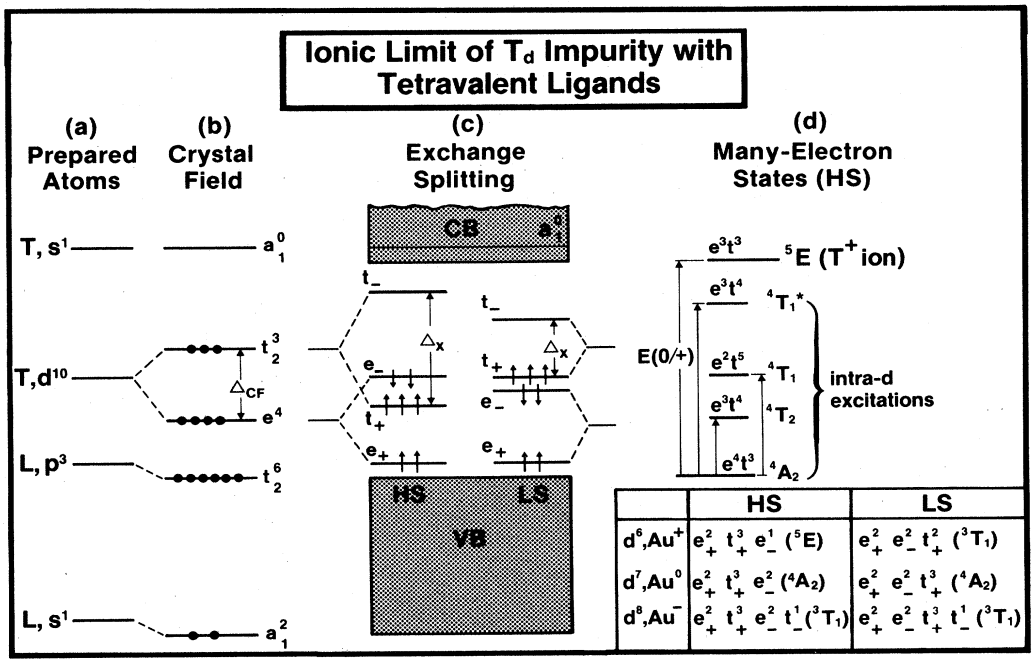


FIG. 2. Application of the Ludwig-Woodbury ionic model to substitutional 11-electron $d$-orbital impurities ($Cu^0$, $Ag^0$, $Au^0$, $Ni^-$, $Pd^-$, $Pt^-$) in a tetravalent host crystal with tetrahedral symmetry (Si,Ge).

upper valence band (VB3) below the empty metal-$s$ conduction band (CB). Hence, the $s$ orbital of the metal atom becomes effectively depopulated in the solid, as it does in the LW model. This picture is substantiated by modern band-structure calculations.[65] In NiO [Fig. 1(b)] the O $2p^4$ atomic level becomes fully occupied in the solid, forming the O $2p^6$ band (VB2, often referred to as the $\sigma$ band), leaving $n+m-2=9$ electrons to the $Ni^{2+}$ $d$ states. These nine electrons fill completely the $t_2$ band but leave the upper $e$ band only half-filled. This open-shell structure gives rise to a series of multiplets[66] that are entirely analogous to the $d \rightarrow d^*$ excitations observed in $3d$ impurities in III-V compound semiconductors,[67] as well as to the magnetic properties of NiO. Finally, the same model applies to the Cu and Ag impurities in alkali halides [Fig. 1(c)], which have been studied recently.[68–71] After the transfer of $M=1$ electrons from the impurity to the lattice, the ten remaining electrons form the $t_2^6 e^4$ impurity levels. The empty impurity $a_1$ and $t_1$ levels remain unoccupied and higher in the band gap. Optical transitions of the $e^4a^0 \rightarrow e^3a^1$ type (giving the $^1E$ singlet and the $^3E$ triplet) or $t^6a^0 \rightarrow t^5a^1$ type (producing the $^1T+{}^3T$ multiplets) are observed,[69,71] in analogy with the free-ion $Cu^+$ $d^{10}s^0 \rightarrow d^9s^1$ excitations. In all cases shown in Fig. 1 the simple LW-type ionic model correctly explains numerous experimental observations and is consistent with the result of subsequent accurate electronic structure calculations.[64,65,68–70] As can be seen from Fig. 1, the essence of the model is that *the ligand orbitals L are assumed to lie below the d orbitals of the transition (T) atom.*

Figure 2 illustrates the application of the LW model to substitutional $N=11$ electron impurities (e.g., $Au^0$, $Cu^0$, $Ag^0$, $Pt^-$, and $Ni^-$) in a tetravalent ($M=4$) host crystal (Si, Ge). As in Fig 1, one assumes that the ligand atomic orbitals $L$ are lower in energy than the $d$ orbitals of the metal impurity $T$. In this case, the $s^1$ and $p^3$ (i.e., $sp^3$) orbitals of the ligand [Fig. 2(a)] form bonding combinations with the corresponding metal orbitals, resulting [Fig. 2(b)] in filled ligand bands of the $a_1^2$ and $t_2^6$ symmetries, respectively (analogous to VB1 and VB2 of Fig. 1). After remaking the broken ligand bonds, $n+m-4=7$ electrons are available to the metal impurity itself, which has now become a Au(4+) species. These seven electrons fill the $t_2$ and $e$ levels in the $e^4t_2^3$ high-spin configuration for the neutral center [or $e^3t^3$ for the positive center and $e^4t^4$ for the negative center; cf. Fig. 2(c)]. The inclusion of exchange interactions results in the Hund's-rule level occupations and multiplet states indicated in the first column (HS) of Fig. 2(d); a LSL-level arrangement (rejected by LW) would result in the multiplets denoted in the second column of Fig. 2(d). The $e_+^2t_+^3e_-^2(^4A_2)$ neutral center has an open shell and can show (charge-conserving) intra-$d$ transitions [Fig. 2(d)], as well as a donor transition $e_+^2t_+^3e_-^2(^4A_2) \rightarrow e_+^2t_+^3e_-^1(^5E)$, in which an $e_-$ electron is ionized to a band state.

### B. Implications of the ionic model for group-IB impurities in Si

The application of the LW model to substitutional Cu, Ag, and Au in silicon (Fig. 2) results in a number of clear predictions:

(i) The $N=11$ state of the system (e.g., $Si:Au^0$, $Si:Pt^-$) is predicted to be a spin $S=\frac{3}{2}$ $^4A_2$ state and hence EPR visible, much like the corresponding $^4A_2$ multiplet states of $Fe^+$ and $Co^{2+}$ in GaAs and GaP that have been observed.[60] Instead, no EPR is obtained for $Si:Au^0$, and the data for $Si:Pt^-$ shows $S=\frac{1}{2}$, which contradicts the model. While it is possible that covalency effects would lead to opposite and, hence, canceling contributions from $p$ and $d$ orbitals, it seems unlikely that this would completely wash out the spectra since similar $^4A_2$ spectra have been clearly observed for $3d$ impurities in other covalent semiconductors.[60] Similarly, the LW model predicts $Au^+$ and $Pt^0$ to be in an EPR-visible $^5E$ state ($S=2$) and $Au^-$ to be in a $^3T_1$ ($S=1$) state, but no such states have been observed for group-IB impurities. Even if one of the EPR spectra were masked by gold complexes, one would expect to see another transition upon doping. Again, no such effect has been observed.

(ii) The model predicts the neutral center to be a Au(4+) or Ag(4+) species, an unprecedented oxidation state for gold or silver.

(iii) The model predicts the donor transition to be a $d^7 \rightarrow d^6$ ionization and the acceptor transition to be a $d^7 \rightarrow d^8$ excitation. Such ionization in the free ions[72] requires an energy in excess of 100 eV. Screening in the solid, although effective,[73] is unlikely to reduce these energies sufficiently to have both confined in the Si band gap, as observed experimentally (around 5.5 and 5.8 eV, respectively, below the silicon vacuum level).

(iv) Since the model places the electrically and optically active electrons in $d$-like localized orbitals, the exchange splitting $\Delta_x$ [Fig. 2(c)] is expected to be large, minimizing (as it does in other systems with large $\Delta_x$, e.g., $3d$ impurities in silicon) Jahn-Teller distortions.

(v) The model predicts that whereas acceptor transitions involve occupation changes in the $t_-$ orbital ($e_-^2t_-^0 \rightarrow e_-^2t_-^1$), donor transitions are predicted to involve changes in the $e_-$-orbital occupation ($e_-^2 \rightarrow e_-^1$), suggesting substantially different cross sections. No such effect has been observed.

Zunger and Lindefelt[73] have shown that the apparent success of the LW model even for $3d$ substitutional impurities of sufficiently large atomic number (e.g., Ni, Cu) is accidental, and that the level ordering of Fig. 2 (ligand states below impurity states) which underlies the LW model is incorrect. The same criticism applies to Ag and Au, as Watkins[74] suggested on the basis of the work of Ref. 73. We elaborate further on this point in Sec. V C. Thermodynamically, the LW model assumes tacitly that the stable $d^{10}$ shell of group-IB impurities is "split" (into $d^7$), and that the bonds made with the ligands can repay the energy lost by destroying the stable $d^{10}$ state. Quantitative calculations[73] show, however, that this is not so. The $d^{10}$ shell is hybridized but does not revert to an open-shell structure. In view of the experimental evidence surveyed in Sec. II and the present analysis (see also Ref. 73), we conclude that the LW model is inappropriate for group-IB impurities in silicon.

### C. s-electron model for Cu, Ag, and Au

In direct opposition to the LW model that correlates optical, magnetic, and electrical activities with the

transition-atom $d$ orbitals, one might take the point of view that these orbitals are chemically inert (corelike) and that group-I$B$ impurities in Si behave essentially as monovalent $s^1$ species. The view of group-I$B$ elements as monovalent atoms is supported by some chemical evidence[75] suggesting that in sufficiently covalent coordination compounds (e.g., AuCN), the Au $5d$ orbitals do not participate in bond formation. At the same time, the substantial differences between Cu, Ag, and Au chemistry and that of their monovalent analogs K, Rb, and Cs, respectively (including differences in bond length, heats of compound formation, crystal structures, etc.), long ago suggested[10(b)] the essential chemical role of the group-I$B$ $nd$ orbitals.

The point of view of the $s$-electron model has been adopted by Lowther[49(a)] and Brotherton and Lowther.[49(b)] In his empirical cluster calculation (which omits the Au $5d$ orbitals from the basis), Lowther finds $Au^-$ to behave as an $s^2$ ion and $Au^0$ to behave as an $s^1$ atom. In particle, the $E(0/+)$ donor transition is ascribed to the emission of a valence-band hole into an $a_1$ impurity level derived from the Au $6s$ orbital [$m(s)$ in the notation of Ref. 47] located just above the valence-band maximum. This suggestion has been motivated[49(b)] by the observation of presumably low entropy factors for the donor transitions, which indicate a small coupling to the lattice (as would be the case if the active level were a delocalized impurity $a_1$ state and not a vacancylike dangling bond). Since, however, the degeneracy factor assumed by Lowther is more than five times smaller than the more recent, reliable value[50] (cf. Sec. II E), his argument does not appear to be tenable. In our previous calculations,[73] as well as in the one reported here, no impurity $a_1$ level ever occurs in the gap for the unrelaxed lattice substitutional site. However, imperfectly converged calculations have been known[76] to produce such spurious $a_1$ levels in the gap, a result that is unmatched by more precise calculations.[73,77,78]

The same point of view or the $s$-electron model has been taken by Kogan and Tolpygo[79] in their pioneering theoretical work on $A$=Cu, Ag, and Au; impurities in silicon and germanium. In their five-atom $Si_4A$ cluster, treated with a minimal-basis valence-bond approach and neglecting the impurity $d$ orbitals, they found the triple acceptors $Au^{3-}$ and $Ag^{3-}$ to be stable (in contradiction with the experimental evidence to date, cf. Sec. II C) and a strongly delocalized impurity orbital. Finally, the point of view of the $s$-electron model is supported also by a recent cluster calculation[80] using the nonrelativistic multiple-scattering $X\alpha$ method (MS $X\alpha$) with the special "Watson sphere" boundary conditions. Alves *et al.*[80] found for substitutional gold that the $Au^0$ $5d$ orbitals were atomically localized and located *below* the valence-band minimum, which indicates their chemical inertness. This result contradicts the photoemission data that place the Au $5d$ electrons in the upper part of the valence band, as is also indicated in the present calculation (cf. Fig. 3). The reason for this anomaly is not fully understood at present. It is, however, most likely related to the creation of an overly attractive potential at the cluster's center due to the removal of electron density from the cluster into the Watson sphere; for extremely localized states as those

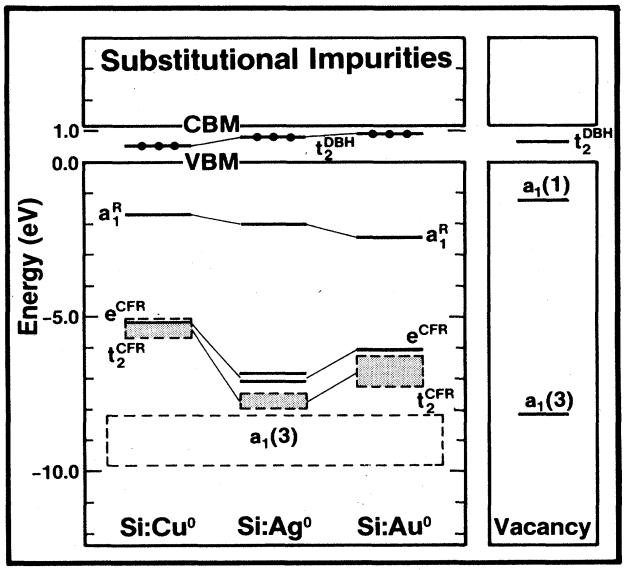


FIG. 3. Energy-level scheme resulting from a self-consistent quasiband crystal-field (QBCF) calculation for neutral unrelaxed substitutional Cu, Ag, and Au impurities in silicon; results for the ideal vacancy are also shown.

arising from these impurities[81] this attractiveness then pulls the $d$ orbitals to spuriously deeper binding energies. We note that similar calculations for Si:Cu also using the MS $X\alpha$ method but employing different boundary conditions[82(a)] (hydrogen terminators which attract charge to the surface of the cluster) correctly reproduce the energies obtained in more recent self-consistent Green's-function results[73] by placing the $d$ levels in the upper part of the valence band, whereas Watson-sphere terminators tend to place the Cu $d$ level *below* the valence-band minimum of semiconductors [i.e., $\sim$13 eV below the result of Ref. 82(a)].[82(b)]. Concomitant with hyperdeep and chemically inactive Au $5d$ orbitals, Alves *et al.*[80] observe a $t_2$ gap level that is exceedingly delocalized for all charge states (only 4% of the charge is in the "impurity sphere"), contains almost no $d$ character, and has consequently a charge-independent orbital energy (hence, the Coulomb repulsion $U\simeq 0$). This leads to the prediction of nearly identical acceptor and donor levels for Si:Au, from which the authors conclude that the experimentally observed transitions could not be caused by a three-charge-state impurity ($Au^+$, $Au^0$, and $Au^-$), but rather are related to some complex.

Our analysis of the $s$-electron model for substitutional group-I$B$ impurities suggests that there is no evidence to support this.

### D. Atomic considerations

To further develop our intuition on group-I$B$ impurities, we present in Table I a collection of some observed and calculated atomic properties: experimental[83] ionization energies $(IP)_\alpha^{expt}$ for excitations from the $\alpha=s$ and $\alpha=d$ orbitals, calculated semirelativistic (SR) ionization energies $(IP)_\alpha^{SR}(LD)$ using the local-density model (LD),

TABLE I. Summary of some experimental and calculated properties of the Cu, Ag, and Au atoms. $(IP)_\alpha^{expt}$ is the experimental (Ref. 83) $\alpha$-orbital ionization energy corresponding to, i.e., $d^{10}s^1 \rightarrow d^{10}s^0$ for $\alpha=s$, and $d^{10} \rightarrow d^9$ for $\alpha=d$. $(IP)_\alpha^{SR}(LD)$ are the corresponding calculated local-density (LD) semirelativistic (SR) ionization energies obtained from the transition-state pseudopotential calculation. $\epsilon_s^{SR}(LD)$ and $\epsilon_d^{SR}(LD)$ are the corresponding LD orbital energies, and $\epsilon_\alpha^{NR}(HF)$ are the nonrelativistic Hartree-Fock (HF) (Ref. 84) orbital energies. All energies are in eV. $\langle r_s \rangle_{LD}$ and $\langle r_d \rangle_{LD}$ are the SR-LD orbital moments, i.e., $\int \psi_\alpha(r) r \psi_\alpha(r) r^2 dr$, and $\langle r_\alpha \rangle_{HF}$ are the NR-HF values (Ref. 84). Both are given in a.u. $r_{BS}$ is the Bragg-Slater (Ref. 85) covalent radius. The electronegativity given is on Pauling's scale. We also give the observed oxidation states, with the less stable ones in parentheses.

| Property | Cu | Ag | Au |
|---|---|---|---|
| $(IP)_s^{expt}$ | 7.73 | 7.58 | 9.22 |
| $(IP)_d^{expt}$ | 20.29 | 21.49 | 20.50 |
| $(IP)_s^{SR}$ | 9.25 | 9.17 | 11.20 |
| $(IP)_d^{SR}$ | 15.73 | 16.86 | 15.64 |
| $\epsilon_S^{SR}(LD)$ | 5.67 | 5.72 | 7.41 |
| $\epsilon_d^{SR}(LD)$ | 8.36 | 10.70 | 10.03 |
| $\langle r_s \rangle_{LD}^{SR}$ | 2.76 | 2.93 | 2.70 |
| $\langle r_d \rangle_{LD}^{SR}$ | 0.97 | 1.37 | 1.57 |
| $\epsilon_S^{NR}(HF)$ | 7.75 | 7.06 | 6.98 |
| $\epsilon_d^{NR}(HF)$ | 20.14 | 19.21 | 17.98 |
| $\langle r_s \rangle_{HF}$ | 2.97 | 3.30 | 3.39 |
| $\langle r_d \rangle_{HF}$ | 0.92 | 1.31 | 1.49 |
| Oxidation states | 2,(1) | 1 | 3,(1) |
| $r_{BS}$(Å) | 1.35 | 1.60 | 1.35 |
| Electronegativity | 1.9 | $\geq 1.9$ | 2.4 |

calculated local-density orbital energies $\epsilon_\alpha^{SR}(LD)$ and orbital moments $\langle r_\alpha \rangle_{LD}$, as well as the corresponding values $\epsilon_\alpha^{NR}(HF)$ and $\langle r_\alpha \rangle_{HF}$ calculated[84] from the nonrelativistic (NR) Hartree-Fock (HF) model. Finally, we give Pauling's electronegativity and the Bragg-Slater[85] (BS) covalent radii $r_{BS}$.

A few observations are apparent. Whereas the nonrelativistic orbital energies [e.g., $\epsilon_\alpha^{NR}(HF)$] are monotonic functions of the atomic number $Z$, showing the usual decrease in both $s$ and $d$ binding energies as $Z$ increases from Cu to Ag and Au, both the observed $(IP)_\alpha^{expt}$ and calculated relativistic ionization energies $(IP)_\alpha^{SR}(LD)$ show a nonmonotonic behavior: silver has the lowest $s$-binding (i.e., ionization) energy and the highest $d$-binding energy. Along with its loose outer orbital, silver has the largest covalent radius $r_{BS}$ and orbital radius $\langle r_s \rangle_{LD}$. Having the deepest (i.e., most inert) $d$ orbitals, its only observed oxidation state is $+1$, whereas both Cu and Au can utilize their $d$ orbitals in bonding, showing higher oxidation states (the most stable being $2+$ for Cu and $3+$ for Au). These phenomena are consequences of relativistic effects, which are most pronounced in gold. Here, the relativistic correction causes the $s$ orbital to contract the most around the nucleus and hence best shield it. Indeed, whereas the nonrelativistic orbital radius $\langle r_s \rangle_{HF}$ shows that the heaviest atom (Au) is also the largest, the relativistic calculation yielding $\langle r_s \rangle_{LD}^{SR}$ shows Au to be the smallest atom in this series. As a result of the effective screening of the gold nucleus by the contracted $s$ orbital, its $s$ electrons become deeper ("corelike") and its $d$ electrons, experiencing additional Coulomb repulsion from this inner $s$ density, have a smaller binding energy than would otherwise be expected. The tightly bound electrons are not easily transferred to other atoms in bond formation, which results in a very large electronegativity for Au. Similarly, the occurrence of loose $s$ electrons but very deep $d$ electrons causes silver to have only the oxidation number 1.

We conclude that a relativistic calculation is necessary for obtaining the correct chemical trends in energies and spatial extent in the *IB* series. Such a calculation (neglecting, however, spin-orbit corrections) is reported in this work. Although the LD calculation used here (cf. Table I) produces the correct trends, we also observe that its ionization energies are too small. This would have been a serious problem were the noble-atom orbitals in the solid isolated in the band gap or below the valence-band minimum (i.e., as localized as in their atomic states). Since we find, however, that the $d$ orbitals participate in bonding inside the valence and that the $s$ orbitals are empty, this is less of a problem. Similarly, the absence of any strong impurity $d$ or $s$ character for the gap levels suggests that the neglect of spin-orbit splitting is not detrimental. This, however, will affect the impuritylike $d$ states inside the host valence band.

### E. Summary

From our analysis of the conceptual models for group-*IB* impurities, we conclude the following.

(i) The Ludwig-Woodbury ionic model, which works well for ionic coordination compounds, contradicts both the experimental data and the level ordering produced by detailed calculations[73] for group-*IB* impurities; the $s$-electron model is not supported by the data.

(ii) In view of the concepts introduced by these models and the questions they raise, we feel that the outstanding theoretical issues are as follows: (a) To what extent do the $d$ electrons influence the properties of the system? (b) Does the system involve open-shell $d$-orbital structures with their attendant many-electron multiplet effects and the suppression of Jahn-Teller distortions, or is the picture of non-$d$-like gap orbitals with their attendant Jahn-Teller distortions and attenuated multiplet effects more appropriate? (c) What is the nature of the orbitals that give rise to the electrical (i.e., donor and acceptor) and magnetic (i.e., EPR) properties? (d) Can a two-level, three-charge-state model explain the data, or is the postulation of complex defects or lattice relaxation *essential* to explain it qualitatively? (e) Are the data for the impurities understandable in light of the *atomic* trends (cf. Table I), or are solid-state effects overriding?

This perspective guided our calculation, which attempts to provide an initial theoretical description of this system.

## IV. METHOD

We have used the self-consistent quasiband crystal-field (QBCF) Green's-function method of Lindefelt and Zunger[86] to solve for both substitutional Ag and Au and interstitial Au impurities in silicon within the local-density approximation. This complements results obtained earlier[73] for the substitutional Cu impurity. We have constructed semirelativistic pseudopotentials (i.e., a single-component wave function with a relativistic potential, not including spin-orbit interactions) using the same procedure previously employed to introduce other core effects into the pseudopotential (e.g., self-interaction-corrected pseudopotentials[87]). Our procedure[87] is analogous to that proposed by Kleinman[88] (producing indeed very similar results), but does not achieve "norm conservation" through manipulation of the potential; instead, this is achieved through the Zunger-Cohen original procedure.[89] We use an exchange coefficient of $\alpha=1$, as before.[73] The resulting (pseudopotential) atomic orbital energies and ionization energies are given in Table I. The QBCF method has been previously tested for the unrelaxed Si vacancy[86] and applied to numerous other problems, including substitutional[73] and interstitial[77] $3d$ impurities in Si, the core exciton[90(a)] and substitutional $3d$ impurities in GaP,[90(b)] and chalcogen impurities in silicon.[91] We will not repeat the details of the method[86] here; the interested reader is referred to these previous publications on this subject. We note that in calculating the levels of the charged states $A^+$ or $A^-$ we extend the integration of the change in charge density up to a distance $R_c$ that assures the electrostatically correct charge of $1/\epsilon_0$ and $-1/\epsilon_0$ for $A^+$ and $A^-$, respectively (where $\epsilon_0$ is the dielectric constant). The same cutoff $R_c$ is used for the neutral state. A small, effective-mass correction for the long-range electrostatic potential (omitted from the Green's-function calculation) is then outside $R_c$ applied to the calculated eigenvalues.

## V. SUBSTITUTIONAL GROUP-I*B* IMPURITIES IN Si

Figure 3 depicts the self-consistently calculated, one-electron energy levels for neutral, unrelaxed, substitutional Cu, Ag, and Au impurities in silicon. For comparison, we also give our previous result[86] for the Si vacancy.

We see that these impurities introduce into the band gap a single level of $t_2$ symmetry termed, in analogy with Ref. 73, the "dangling-bond hybrid" (DBH), as well as two levels inside the valence band, one of $t_2$ and the other of $e$ symmetry. They are termed "crystal-field resonances" (CFR) for reasons that will become clear later. In addition, weaker $a_1$ resonances ($R$) appear in the upper part and near the bottom of the valence band. The $t_2^{\mathrm{DBH}}$ gap level is occupied by three electrons in the neutral state of the impurity (two electrons for the $A^+$ state and four electrons for the $A^-$ state). Their energies for the neutral centers are calculated to be $E_v+0.57$ eV for Si:Cu, $E_v+0.63$ eV for Si:Ag, and $E_v+0.72$ eV for Si:Au. The uncertainty in these values, due to our truncation procedure and effective-mass correction is estimated at $\pm 0.05$ eV or less. Table II provides a decomposition of the electronic charge $q_i$ enclosed within a sphere of nearest-neighbor radius (4.44 a.u. in Si) around the impurity, for each of the impurity-induced states $i$, into its angular momentum $l$ components. The results are normalized to one electron. We now proceed with the identification of these calculated impurity-induced states.

### A. Crystal-field resonances

The occupied $t_2^{\mathrm{CFR}}$ and $e^{\mathrm{CFR}}$ levels appear as resonances around the center of the valence band, and show a nonmonotonic ordering (Ag is the deepest) and an octahedral level arrangement ($e^{\mathrm{CFR}}$ above $t_2^{\mathrm{CFR}}$). The total electronic charge enclosed in these levels within a nearest-neighbor sphere ($q_i$ in Table II) shows the $e^{\mathrm{CFR}}$ state to be over 90% localized and the $t_2^{\mathrm{CFR}}$ state to be 70—80% localized. The degree of localization of both levels decreases somewhat with atomic number $Z$, paralleling the increased size of the $nd$ atomic orbitals (cf. $\langle r_d \rangle_{\mathrm{LD}}^{\mathrm{SR}}=0.97$, 1.37, and 1.57 a.u., respectively, for Cu, Ag, and Au in Table I). The relative widths of these resonances parallel their localization, the $t_2^{\mathrm{CFR}}$ being wider than the $e^{\mathrm{CFR}}$ state. An angular momentum decomposi-

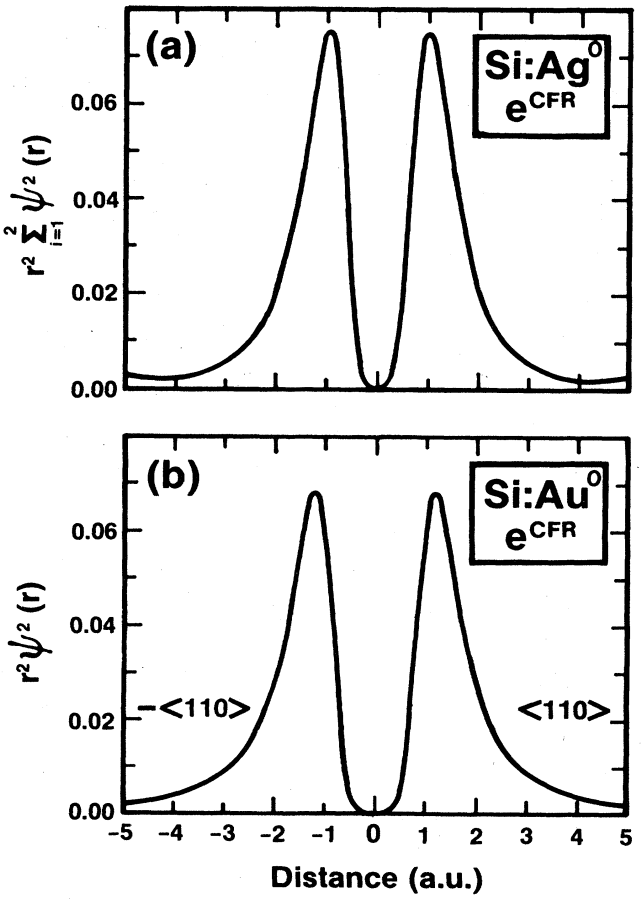


FIG. 4. Radial charge densities in the $\pm\langle 110\rangle$ crystal directions for the $e^{\mathrm{CFR}}$ states in the Si valence band for the neutral impurities Ag and Au. Results for Si:Cu have been presented elsewhere (Refs. 73 and 86).

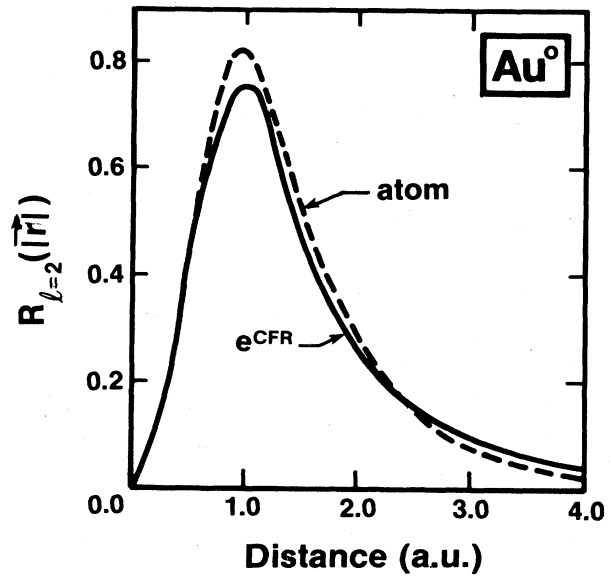


FIG. 5. Radial part of the $l=2$ ($d$-orbital) component of the $e^{CFR}$ state of Si:Au$^0$, compared with the atomic $5d$ pseudo-orbital.

tion (Table II) shows the $e^{CFR}$ level to be pure $d$-like, whereas the $t_2^{CFR}$ level is strongly $d$-like, with some admixture of $p$ character from the tails of the ligand $sp^3$ orbitals. Figure 4 depicts the radial charge density of the $e^{CFR}$ wave function (for Ag we sum the densities of the two resonances) and for Si:Ag and Si:Au (results for Si:Cu were presented previously[73]), showing some delocalization with increasing atomic number, much like the atomic effect (cf. $\langle r_d \rangle_{LD}^{SR}$ in Table I) in going from $3d$ to $4d$ and $5d$. Figure 5 compares the $l=2$ ($d$ component) of the $e^{CFR}$ resonance of Si:Au$^0$ with the atomic $5d$ pseudoorbital of gold. It shows a very slight solid-state effect of delocalization. A similar conclusion can be drawn from the $t_2^{CFR}$ wave function.

There can be no doubt that the $e^{CFR}$ and $t_2^{CFR}$ resonances are the descendants of the free-atom $nd$ orbitals of the group-I$B$ atom, being slightly hybridized and perturbed (i.e., split) by the crystalline field (hence, the term CFR). This contradicts the ionic model (cf. Sec. III A) that places the atomic $d$ orbitals inside the band gap (hence, suggesting their participation in optical and electrical activity) and with the $s$-electron model (cf. Sec. III B) that places these $d$ states below the valence-band minimum (hence, assuming their complete inertness). The atomic fingerprint of these CFR states is their ordering; much like relativistic effects increase the $d$-orbital binding energy of Ag relative to that of Cu and Au (cf. Table I), so do these effects produce the same distinct ordering in the solid (Fig. 3). The position of these levels is consistent with the photoemission data (cf. Sec. II G) that place them near the center of the valence band (however, no precise comparison of their energies can be made since theory lacks spin-orbit splitting and orbital relaxation effects and experiment pertains to a high impurity concentration). Because of their relatively high localization, we predict that optical excitations from the fully occupied $e^{CFR}$ and $t_2^{CFR}$ levels will produce impurity-bound excitons, i.e., a hole in either of these levels will lead to a more attractive central-cell potential, hence, a splitting of an exciton level from the conduction band into the gap. The localized-to-itinerant excitations from these levels into the conduction band are subject to large orbital relaxation shifts and are expected to produce singlet-triplet pairs (i.e., $^1E$ and $^3E$ for excitation of $e^{CFR}$, $^1T$ and $^3T$ for excitations of $t_2^{CFR}$) completely analogous (but in reversed order) to the situation occurring for noble-atom impurities in alkali halides[68–71] [cf. Fig. 1(c); note that in the latter case these

TABLE II. Orbital character of the main impurity-induced states in neutral substitutional Si:Cu, Si:Ag, and Si:Au. The total orbital charges $q_i$ are normalized to one.

| System | Level | Total charge $q_i(e)$ | $s$ charge $q_{il}=0(\%)$ | $p$ charge $q_{il}=1(\%)$ | $d$ charge $q_{il}=2(\%)$ |
|---|---|---|---|---|---|
| Si:Cu$^0$ | $a_1^R$ | 0.35 | 94 | 0 | 0 |
| | $e^{CFR}$ | 0.94 | 0 | 0 | 100 |
| | $t_2^{CFR}$ | 0.80 | 0 | <2 | 97 |
| | $t_2^{DBH}$ | 0.38 | 0 | 76 | 22 |
| Si:Ag$^0$ | $a_1^R$ | 0.29 | 97 | 0 | 0 |
| | $e^{CFR}$ | 0.90 | 0 | 0 | 100 |
| | $t_2^{CFR}$ | 0.70 | 0 | <2 | 94 |
| | $t_2^{DBH}$ | 0.41 | 0 | 80 | 18 |
| Si:Au$^0$ | $a_1^R$ | 0.13 | 97 | 0 | 0 |
| | $e^{CFR}$ | 0.90 | 0 | 0 | 100 |
| | $t_2^{CFR}$ | 0.67 | 0 | 3 | 95 |
| | $t_2^{DBH}$ | 0.44 | 0 | 82 | 18 |

are the lowest-energy transitions]. The $e^{CFR}$-$t_2^{CFR}$ energy separation constitutes the crystal-field splitting $\Delta_{CF}$ (unlike the Ludwig-Woodbury assignment that identifies the $t_2^{DBH}$-$e^{CFR}$ separation as $\Delta_{CF}$). We conclude that the $d$ orbitals of the group-I*B* impurities are not directly active in electrical, optical, and magnetic excitations. (They do affect, however, through a "feedback effect," the active gap levels as discussed in Sec. V E.) We note further that because of hybridization with the ligands, the $t_{CFR}^6 e_{CFR}^4$ configuration cannot be considered a "$d^{10}$ system,"[74,80] in the same way that the valence band of CuCl [VB2 in Fig. 1(a)] cannot be considered a Cl $p^6$ band. Part of the $d$ character of the group-I*B* impurities ($p$ character of chlorine in CuCl) is pushed into the levels above this valence band and replaced by Si $p$ (Cu $3d$,$4p$) character. This hybridization of the I*B* impurity atom with the host ligands through the $t_2^{CFR}$ state is likely to provide most of the binding energy of the substitutional impurity to the lattice (the gap level $t_2^{DBH}$ is *antibonding*, hence its occupation *destabilizes* the lattice). We suspect that the low diffusion constant of the substitutional group-I*B* impurities (even lower than that of the vacancy, which has $t_2^{DBH}$ but no $t_2^{CFR}$ states) is mainly a consequence of the formation of some metal-silicon bonds through the $t_2^{CFR}$ states.

### B. Dangling-bond hybrids

The antibonding counterpart of the $t_2^{CFR}$ state appears in the band gap as a dangling-bond hybrid. It is considerably more delocalized (localization parameters of 38 to 44%; cf. Table II) than the bonding state, yet it is somewhat more localized than the vacancy state (35%; cf. Table IV in Ref. 86). This gap level is a $p$-$d$ hybrid, showing a relative increase in the $p$ character with increasing impurity atomic number. Therefore, we view this state as a hybrid between the silicon dangling bonds and the impurity central orbitals (hence the term DBH). Its delocalization is a consequence of its orthogonality to the deeper, localized $t_2^{CFR}$ state. Despite a ~5- eV energy separation between the two, this orthogonality relation provides a coupling between the two states: the $t_2^{DBH}$ states are higher in energy than the corresponding vacancy state, partially due to this bonding-antibonding orthogonality repulsion (this is basically the reason why no double acceptor is expected for substitutional group-I*B* impurities in silicon). One should also note that as this $t_2^{DBH}$ level rises slightly in energy from Si:Cu$^0$ to Ag$^0$ to Au$^0$, the $a_1$ resonance (characteristic of the rebonding of the "vacancy" dangling bonds) moves *down* in energy, so that the center of gravity for the dangling-bond hybrid remains approximately constant (cf. Fig. 3). It is interesting to observe that the $a_1$-$t_2$ splitting increases from the vacancy to the Cu impurity, indicating some remaking of

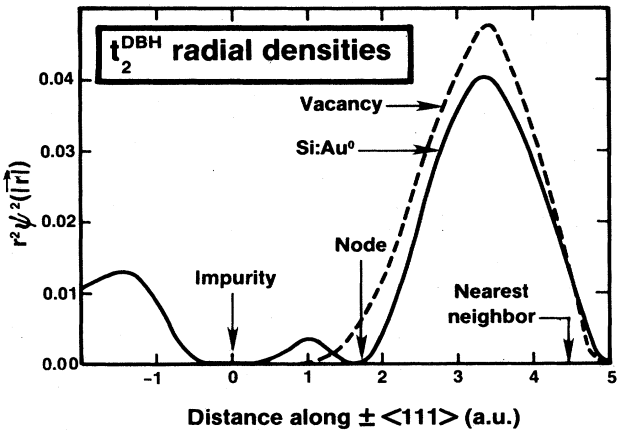


FIG. 6. Radial charge densities in the $\pm\langle 111\rangle$ directions for the $t_2^{DBH}$-gap state of the Si:Au$^0$ system (solid line) and for the $t_2^{DBH}$-gap state of the silicon vacancy (Ref. 86) (dashed line), both normalized to one.

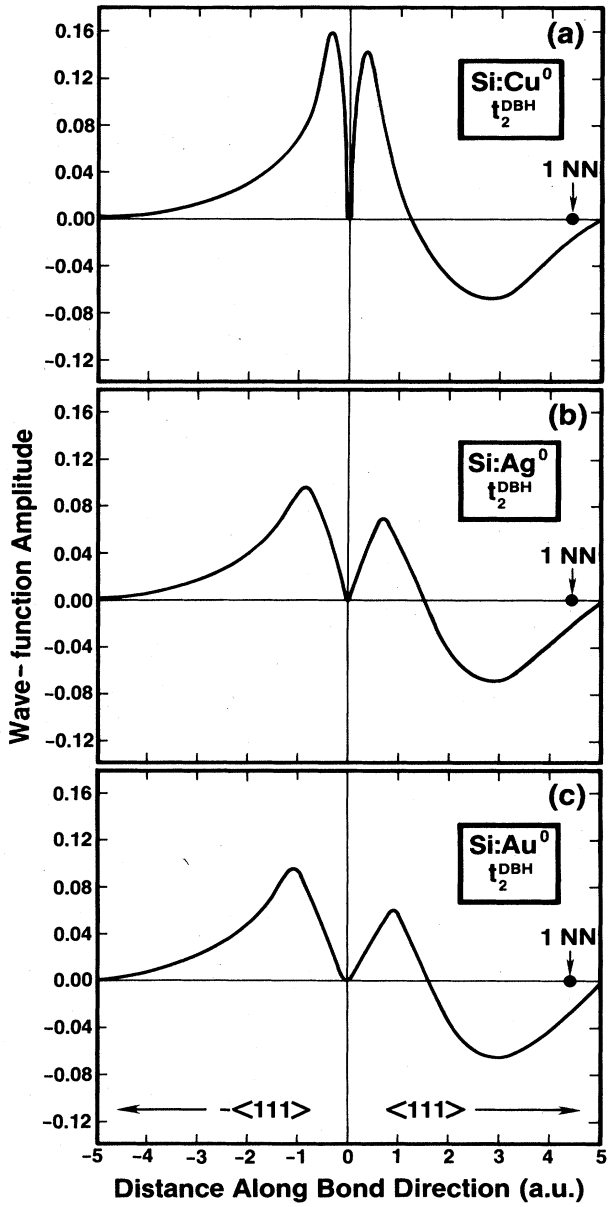


FIG. 7. $t_2^{DBH}$ wave functions of (a) Si:Cu$^0$, (b) Si:Ag$^0$, and (c) Si:Au$^0$.

tetrahedral bonds. It continues to increase from $Cu^0$ to $Ag^0$ to $Au^0$ (whereas, if the bonds were completely "healed," as in the case of a Si or P central atoms, the $a_1$-$t_2$ splitting would be $\sim 12$ eV). Figure 6 displays a comparison between the radial charge density of the $t_2^{DBH}$ state of Si:$Au^0$ and the corresponding dangling-bond hybrid of the silicon vacancy.[86] The significant difference between the two[73] is the occurrence of the antibonding node in Si:$Au^0$ *well inside the central cell* (at a distance of 1.26, 1.53, and 1.65 a.u. from the impurity for Si:$Cu^0$, Si:$Ag^0$, and Si:$Au^0$, respectively, paralleling the increase in size of the *nd* atomic orbitals with the principle quantum number *n* shown in Table I). In contrast, the vacancy $t_2^{DBH}$ state does not carry an "impurity signature;" its node is well outside the nearest-neighbor shell (cf. Fig. 10 in Ref. 73). Furthermore, whereas the vacancy $t_2^{DBH}$ state has a vanishingly small amplitude in the $-\langle 111 \rangle$ direction (towards the interstitial site), the $t_2^{DBH}$ of the group-I*B* impurities has a considerable amplitude in this volume. Figure 7 displays the trends in the $t_2^{DBH}$ wave functions for Si:Cu, Si:Ag, and Si:Au. While they show a general similarity to one another, they also exhibit the unmistakable fingerprint (i.e., node position) of the central impurity atom. Their common dangling-bond character may explain the "universality" of the emission rates observed by Lang *et al*,[40] and the vacancylike character suggested by Van Vechten and Thurmond.[24]

### C. Implications of the electronic structure: the hybridized model

The $t_2^{DBH}$ level has no counterpart in the LW ionic model, as LW had tacitly presumed the host ("ligand") states to be *deeper* in energy than the impurity *d* states (cf. Figs. 1 and 2), which is appropriate only for highly electronegative ligands in oxides. In contrast, our results suggest that these ligand-derived $t_2^{DBH}$ orbitals (not the group-I*B* *d* orbitals $t_2^{CFR}$ and $e^{CFR}$) control the optical, magnetic, and electrical properties of the system. The energy-level scheme appropriate for this system is the one discussed previously by Zunger and Lindefelt.[73,92] There, the $sp^3$-ligand orbitals are at *higher energy* than the group-I*B* atom *d* orbitals, leading to the formation of a low-lying, occupied *bonding* $t_2^{CFR}$ state, and a partially empty *antibonding* $t_2^{DBH}$ orbital in the band gap. The nonbonding $e^{CFR}$ state lies between the two. The chemical trends expected from such a model along a row in the Periodic Table (e.g., the $e^{CFR}$ orbital becomes optically and electrically active for impurities near the center of the 3*d* series) have been discussed elsewhere.[73,92] The implications of this model for group-I*B* impurities in silicon are the following.

(i) Due to the substantial spatial extent of the $t_2^{DBH}$-gap orbitals, exchange splitting ($\Delta_x$) and multiplet effects are expected to be small, in contrast with the situation for the main-group 3*d* impurities.[67,73] This suggests that lattice distortion (e.g., Jahn-Teller) effects, which can be suppressed by the strong exchange interactions in main group 3*d* impurities, would be significant for group-I*B* impurities. *Hence, we predict a low-spin-like (LSL)-level arrangement, in contrast to the ionic model, which predicts a high-spin-like (HSL)-level ordering.* A similar transition from a LSL-to a HSL-level arrangement has recently[90(b)] been predicted to occur both at the high-*Z* (Zn, Cu) and the low-*Z* (V,Ti) impurity limit for GaP:3*d*. Recently,[78(b)] Kutagama-Yoshida and Zunger predicted a similar LS for interstitial Si:$V^0$, Si:$Ti^0$, Si:$V^+$, and Si:$Co^{2+}$.

(ii) The electrical activity is related to depopulation (donor transitions) or population (acceptor transitions) of the hybridized gap levels which are split, through lattice distortions, from the $t_2^{DBH}$ levels. Unlike the case of the light 3*d* impurities in Si,[73] these transitions are largely unrelated to the *d* orbitals.

(iii) The multiplet structure and its underlying spin values derived from the ionic model for group-I*B* impurities [Fig. 2(d)] are irrelevant to the EPR of this system. Indeed, no $S=\frac{3}{2}$ is expected for Si:$Au^0$ or Si:$Pt^-$. Instead, the expected spin states are those derived from the lattice-distorted split-off $t_2^{DBH}$ levels. Since all conceivable Jahn-Teller distortions of a $t_2^3$ level[74] produce a lower, doubly occupied spin-paired ($a_1$-like) level and a singly occupied level ($b_1$- or $b_2$-like) above it, one expects $S=\frac{1}{2}$ for Si:$Au^0$ and Si:$Pt^-$, and $S=0$ (i.e., EPR-invisible) for both Si:$Au^+$ and Si:$Au^-$. Whereas in the ionic model, an EPR signal was expected[55,59] to be detected for all charge states [cf. the table in Fig. 2(d)], i.e., for all doping levels, our conclusion here suggests that if complexes do not mask the EPR of the isolated center, an $S=\frac{1}{2}$ spectra is expected only for Si:$Au^0$ (intrinsic material), i.e., for Fermi energies below the acceptor state ($\sim E_v+0.63$ eV) but above the donor state ($\sim E_v+0.35$ eV). We note, however, that even for this range of Fermi energies only a small isotropic central hyperfine constant *A* may occur in Si:Au: gap orbitals of $b_1$ or $b_2$ symmetries have a node at the impurity site and hence do not contribute to *A*. Essentially all of the isotropic contribution to *A* would then come from spin polarization of the impurity's core *s* orbitals by the gap-level and valence-band resonances. However, the near $d^{10}$ character of the VB resonances of substitutional gold in Si (as opposed to the $d^9$ character of the valence-band resonances in Si:$Pt^-$) suggests that this contribution might be small, in contrast to the case of 3*d* impurities (or Si:$Pt^-$) leading to a small istropic contribution to *A*. Most of the signal would then be anisotropic. Furthermore, since all of the gold appears as the isotope with nuclear spin $\frac{3}{2}$ (whereas in Pt, 66% of the metal has zero nuclear spin and 34% has $I=\frac{1}{2}$), one expects twice as many satellite EPR lines in Au relative to Pt, creating a broader band in the former case. (This point has been discussed with E. Weber; we are grateful for his suggestions.) These factors combine to make the EPR of gold difficult to observe.

It is interesting to speculate on the likely form of lattice distortions around group-I*B* impurities in silicon. The isoelectronic mapping between these centers and the Si vacancy ($V^{2-} \leftrightarrow A^-$), ($V^- \leftrightarrow A^0$), ($V^0 \leftrightarrow A^+$), ($V^+ \leftrightarrow A^{2+}$), and ($V^{2+} \leftrightarrow A^{3+}$) would suggest $A^{3+}$ to be undistorted, $A^{2+}$ to have a tetragonal distortion like the (stronger) one in $A^+$, and $A^0$ would then have a tetragonal distortion with a trigonal component. These considerations ignore, however, the structural significance of the chemically active $t_2^{CFR}$ states that are missing in the silicon vacancy.

These states, as discussed in Sec. V A, are bonding combinations; hence, they contribute to the binding of the impurity to the lattice and determine its equilibrium conformation. They carry further the distant signature of the particular group-I*B* atom involved. The structural chemistry of these elements[93] suggests three predominant bonding forms: (i) Ionization of the outer *s* electron, which results in an inert $d^{10}$ closed shell with essentially no bonds. This form exists predominantly in electrolyte solutions. We will see (Sec. VI) that this is the most likely form of *interstitial* group-I*B* elements in Si. (ii) Utilization of the *s* orbital in combination with a single *p* orbital to form two collinear *sp* bonds in double coordination. This form is very rare for Cu(I) (it exists in $Cu_2O$), but is the dominant structural form for Ag(I) and Au(I), e.g., in AgCN, AuCN, and AuI. (iii) Utilization of the *s* orbital plus three *p* orbitals, to form fourfold $sp^3$ (or sixfold) coordinated tetrahedral (or octahedral) structures. This form is extremely rare for Au(I), but it exists both for Cu(I) [forming the zinc-blende compounds CuCl, CuBr, CuI, and $Cu(CN_4)^{3-}$] and for Ag(I) (forming rocksalt compounds like AgF, AgCl, and AgBr).

These considerations suggest that there is no unique, vacancylike distortion for all three centers. It appears that (i) Au is likely to form two nearly collinear bonds in Si, i.e., the impurity approaches two Si sites, increasing their tetrahedral angle towards 180°, and leaving the other two Si atoms to rebond among themselves; (ii) Cu is likely to maintain a distorted structure close to the fourfold coordinated zinc-blende structure (i.e., near substitutional); and (iii) Ag is likely to show a combined distortion pattern and perhaps exist in Si in more than one structural form. It is expected to have the lowest binding energy to the lattice, relative to Cu and Au. In addition, the strong dependence of the group-I*B* ionic radii on their charge states[94] suggests a similar dependence of the reconstruction amplitudes on charge (although not as much as in ionic compounds, due to the charge self-regulating response[92] of Si). Detailed relaxation calculations would be needed to establish the precise forms of these distortions, and no simple answers would be expected.

### D. Electrical levels

One of our foregoing conclusions [item (ii) in Sec. V C] suggests that the electrical levels should be calculated as transitions from the distortion-split gap level to the band-edge states. [We denoted here the split gap level by the general notation $a_1^2(b_1b_2)^1$]. Since our present calculation assumes an undistorted lattice, we calculate directly only the vertical (ver in subscript) transition energies

$$E_{\rm ver}^{3,4}(0/-)=E_{\rm tot}(t_{\rm DBH}^4)-E_{\rm tot}(t_{\rm DBH}^3)$$

and

$$E_{\rm ver}^{3,2}(0/+)=E_{\rm tot}(t_{\rm DBH}^3)-E_{\rm tot}(t_{\rm DBH}^2)\ .$$

We denote the relaxation corrections to them as $\Delta E_R^{3,4}(0/-)\equiv\Delta E(b^1/b^2)$ and $\Delta E_R^{3,2}(0/+)\equiv\Delta E(b^0/b^1)$. Here, $E_{\rm tot}(t_{\rm DBH}^N)$ denotes the total energy of the system, calculated self-consistently for $N$ electrons in the $t_2^{\rm DBH}$-gap level. The total acceptor energy is then $E(0/-)=E_{\rm ver}^{3,4}(0/-)+\Delta E(b^1b^2)$ and the total donor energy is $E(0/+)=E_{\rm ver}^{3,2}(0/+)+\Delta E(b^1/b^0)$. The Mott-Hubbard Coulomb repulsion[67] is

$$U=[E_{\rm ver}^{3,4}(0/-)-E_{\rm ver}^{3,2}(0/+)]+[\Delta E(b^1/b^2)-\Delta E(b^1/b^0)]\equiv U_{\rm ver}+\Delta U_R\ ,$$

where the first term represents the usual vertical ("Hubbard") $U$ for the undistorted lattice and $\Delta U_R$ denotes the relaxation correction to it. We calculate the vertical ionization energies from the transition-state construct (i.e., $3\frac{1}{2}$ and $2\frac{1}{2}$ electrons in the $t_2^{\rm DBH}$ level for the acceptor and donor transitions, respectively). Assuming that the energy of the gap level changes linearly with occupation in this range, we find (in eV) for Si:Au

$$E(0/-)=(E_v+0.88)+\Delta E_R(b^2/b^1)\ ,$$

$$E(0/+)=(E_v+0.56)+\Delta E_R(b^1/b^0)\ ,$$

and for Si:Ag

$$E(0/-)=(E_v+0.76)+\Delta E_R(b^2/b^1)\ ,$$

$$E(0/+)=(E_v+0.5)+\Delta E_R(b^1/b^0)\ .$$

The effective Coulomb repulsion energies are then

$$U(\mathrm{Au}^0)=0.32+[\Delta E_R(b^2/b^1)-\Delta E_R(b^1/b^0)]$$

and

$$U(\mathrm{Ag}^0)=0.26+[\Delta E_R(b^2/b^1)-\Delta E_R(b^1/b^0)]\ .$$

A comparison with the experimental data surveyed in Sec. II C shows that the calculated *vertical* transition energies are about 0.15—0.25 eV above the *equilibrium* relaxed thermal transition energies, suggesting that lattice distortions $\Delta E_R$ lower the energy by approximately a constant amount of 0.15—0.25 eV for all states. If the suggestion of Morooka *et al.*[22(c)] that high-temperature Si:Au is unrelaxed but the low-temperature Si:Au is relaxed is valid, we would predict the former to have higher donor and acceptor energies (by $\Delta E_R$) then the latter. This awaits experimental testing. The near independence of the *differences* of relaxation corrections on occupations suggests that our values for $U_{\rm ver}$ are close to the observed (relaxed) values of 0.28 and 0.32 eV for Si:Au and Si:Ag, respectively. We find the Au acceptor and donor to be slightly *above* the Ag acceptor and donor, in agreement with the experimental trend.

The significant conclusion here is that our model shows that both the observed acceptor and the donor transitions can arise from the same impurity center (if a similar and physically plausible relaxation correction is applied). This contradicts the conclusions drawn previously[80] from a cluster model, suggesting that $U\simeq 0$ and that the donor and acceptor transitions could not be related to the same center. Our result further contradicts the suggestion of Lowther[49(a)] that lattice relaxation is *essential* to explain the amphoteric nature of these defects. Although we *predict* that relaxation will occur, (cf. Sec. V C), we do not find it essential to explain the amphoteric behavior of the center.

TABLE III. Population analysis of the ground state of substitutional Si:Cu$^0$ (Refs. 73 and 86), Si:Ag$^0$, and Si:Au$^0$. For comparison, the results for the silicon vacancy (Ref. 86) are also given.

| $l$ | $Q_l^{a_1}$ | $Q_l^e$ | $Q_l^{t_1}$ | $Q_l^{t_2}$ | $Q_l$ | $l$ | $Q_l^{a_1}$ | $Q_l^e$ | $Q_l^{t_1}$ | $Q_l^{t_2}$ | $Q_l$ |
|---|---|---|---|---|---|---|---|---|---|---|---|
| | | | Si:Cu | | | | | | Si:Cu | | |
| 0 | 1.709 | 0.000 | 0.000 | 0.000 | 1.709 | 0 | 1.824 | 0.000 | 0.000 | 0.000 | 1.824 |
| 1 | 0.000 | 0.000 | 0.000 | 2.978 | 2.978 | 1 | 0.000 | 0.000 | 0.000 | 2.783 | 2.783 |
| 2 | 0.000 | 4.293 | 0.000 | 6.909 | 11.202 | 2 | 0.000 | 4.202 | 0.000 | 6.657 | 10.859 |
| 3 | 0.141 | 0.000 | 0.453 | 0.156 | 0.750 | 3 | 0.138 | 0.000 | 0.406 | 0.144 | 0.688 |
| 4 | 0.016 | 0.086 | 0.070 | 0.189 | 0.361 | 4 | 0.017 | 0.081 | 0.066 | 0.186 | 0.350 |
| $Q^\alpha$ | 1.866 | 4.379 | 0.523 | 10.232 | 17.000 | $Q^\alpha$ | 1.979 | 4.283 | 0.472 | 9.770 | 16.504 |
| | | | Si:Ag | | | | | | Si vacancy | | |
| 0 | 1.737 | 0.000 | 0.000 | 0.000 | 1.737 | 0 | 1.516 | 0.000 | 0.000 | 0.000 | 1.516 |
| 1 | 0.000 | 0.000 | 0.000 | 2.729 | 2.729 | 1 | 0.000 | 0.000 | 0.000 | 2.136 | 2.136 |
| 2 | 0.000 | 4.268 | 0.000 | 6.721 | 10.989 | 2 | 0.000 | 0.307 | 0.000 | 0.979 | 1.286 |
| 3 | 0.142 | 0.000 | 0.416 | 0.146 | 0.704 | 3 | 0.167 | 0.000 | 0.309 | 0.147 | 0.623 |
| 4 | 0.016 | 0.083 | 0.066 | 0.182 | 0.347 | 4 | 0.024 | 0.116 | 0.082 | 0.227 | 0.449 |
| $Q^\alpha$ | 1.895 | 4.351 | 0.482 | 9.778 | 16.506 | $Q^\alpha$ | 1.707 | 0.423 | 0.391 | 3.489 | 6.010 |

### E. Charge distribution

Having established the reasonableness of our calculated energy-level scheme, we now turn to the description of the bonding mechanisms implied by it. In Table III we give a population analysis of all occupied states for Si:Au$^0$, Si:Ag$^0$, and Si:Cu$^0$ in their ground states. We denote[86] by $Q_l^\alpha$ the electronic charge contributed to the impurity central cell (i.e., enclosed within a sphere of nearest-neighbor radius) by the $l$th angular momentum component ($s$, $p$, $d$, $f$, and $g$ for $l=0$, 1, 2, 3, and 4, respectively) of all occupied states belonging to the $\alpha$th representation ($\alpha=a_1$, $t_2$, $e$, and $t_1$). These orbital representation charges[73] determine, for example, how $p$-like are all $t_2$ states ($Q_{l=1}^{t_2}$), or how $d$-like are all $e$ states ($Q_{l=2}^{e}$), etc. Summing $Q_l^\alpha$ over all representations $\alpha$ produces the orbital occupation number $Q_l$. They determine how much total $p$ character ($Q_{l=1}$) or $d$ character ($Q_{l=2}$) the impurity has in its ground state. Finally, summing $Q_l$ over all angular momentum components $l$ produces the total electronic charge $Q_{\rm tot}$ on the impurity.

These quantities represent both the charge that comes from the impurity atom and the ligand charge that penetrates the central cell. To obtain the effective impurity charges from the impurity alone, we then subtract from $Q_l^\alpha$, $Q_l$, and $Q_{\rm tot}$ the corresponding quantities calculated for the Si vacancy (Table III). This produces the effective impurity charges $\Delta Q_l^\alpha$, $\Delta Q_l$, and $\Delta Q_{\rm tot}$, respectively. They can be calculated by taking the corresponding differences in Table III.

The following conclusions are obvious from this population analysis.

(i) The $a_1$ states are essentially $s$-like (with small $f$ and $g$ components), the $e$ states are all $d$-like, and the $t_2$ states are divided in a 1:2.5 proportion between $p$ and $d$ character. Clearly, the $t_2$ states constitute the main hybridization channel.

(ii) From the $Q_l$ values, one sees that the total $s$ character ($Q_{l=0}$) *increases* from Cu to Ag and Au (a relativistic effect) and that, in response, the total $p$ character ($Q_{l=1}$) *decreases* in the same direction.

(iii) The representation charges $Q^\alpha$ indicate that the $a_1$, $e$, $t_2$, and $t_1$ representations contribute about 12%, 26%, 60%, and 2%, respectively, to the total impurity charge $Q_{\rm tot}$. Again, $t_2$ is the dominant bonding channel.

(iv) The vacancy is seen to have about six electrons ($Q_{\rm tot}$) in its central cell. Relative to this, the Si:Cu$^0$, Si:Ag$^0$, and Si:Au$^0$ centers have in their central cell *extra* ($\Delta Q_{\rm tot}$) 11.0, 10.5, and 10.5 electrons. Since the valence $n+m$ of the atomic $d^{10}s^1$ configuration is 11, this means that Cu in Si is essentially neutral in its central cell, whereas the impurities Ag and Au with the more extended outer orbits have about 0.5$e$ of their 11 valence electrons delocalized outside the central cell. Almost all of this lost charge can be traced to the $t_2^{\rm CFR}$ resonances: comparing Si:Cu with Si:Au, the $t_2^{\rm CFR}$ of the latter loses 0.93$e$, but about 0.4$e$ are returned to the central cell by valence-band states.

(v) The effective orbital configurations $\Delta Q_l$ of the impurities are Cu $s^{0.19}p^{0.84}(dfg)^{9.95}$, Ag $s^{0.22}p^{0.59}(dfg)^{9.68}$, and Au $s^{0.3}p^{0.65}(dfg)^{9.54}$, showing a depopulation of the metal $s$ and $d$ orbitals relative to the atomic ground state, and some bonding, induced through the population of the $p$ orbitals. The population of the $s$ orbitals increases progressively from Cu to Ag and Au, whereas the $d$ orbitals feed back by reducing their occupation. The $l\geq 2$ shell contains less than ten electrons; hence, although the $t_2^{\rm CFR}$ and $e^{\rm CFR}$ orbitals are fully occupied, they do not represent a $d^{10}$ closed shell.

We have similarly computed the *changes* in the charge distribution in Si:Au$^q$ caused by ionization of this center (resulting in formal charge $q$). For instance, upon removing $\frac{1}{2}$ electron from the triply-occupied $t_2^{\rm DBH}$ level of Si:Au$^0$ (forming thereby the $q=\frac{1}{2}$ center) the contribution of this level to the impurity charge drops by $-0.27e$. However, we find that in response to this ionization, the

$e^{CFR}$ and $t_2^{CFR}$ valence-band levels become slightly more deeply bound, with more localized wave functions. This enhanced localization around the impurity contributes an additional $0.05e$ and $0.20e$, from the $e^{CFR}$ and $t_2^{CFR}$ states, respectively, to the impurity charge, cancelling together a total of $0.25e$ out of the $-0.27$ electrons removed from the gap level. Hence, the physical charge on the impurity drops only by $0.04e$ for each electron removed from the gap level in a donor transition (or $\partial\Delta Q_{tot}/\partial q = 0.04$). This near independence of the impurity charge on its formal charge state $q$ is a consequence of the self-regulating response[92] of the valence-band resonances (CFR) to external perturbations (i.e., ionizations). It explains the small effective $U$ in the solid: the atomic value $U_0$ is renormalized in the solid by $(\partial\Delta Q_{tot}/\partial q)^2 U_0$. The existence of a nearly constant impurity charge for all formal charge states $Au^+$, $Au^0$, and $Au^-$ clearly conflicts with the notion underlying the ionic model [cf. Fig. 2(d)].

### F. Summary of results for the substitutional impurities

Our self-consistent calculation for unrelaxed substitutional Cu, Ag, and Au impurities in different charge states in silicon suggests the following conclusions.

(i) The substitutional model shows that these impurities form a two-level (donor and acceptor) three-charge-state ($A^+$, $A^0$, and $A^-$) amphoteric system, where both the donor and the acceptor transition evolve from the same center.

(ii) The undistorted system is characterized by two valence-band resonances, $e^{CFR}$ and $t_2^{CFR}$, with energies approximately at the center of the valence band, and a $t_2^{DBH}$ gap level. The former are the direct descendants of the atomic *nd* orbitals, slightly perturbed and split by the crystal field. The nonmonotonic chemical trend in their binding energies reflects the (relativistic) atomic trend. These states cannot be viewed as a $d^{10}$ closed shell: while fully occupied, they contain less than 10 *d* electrons. Optical excitations of these states to the conduction band are predicted to produce an impurity-bound core exciton as well as multiplet structure (in pairs of singlets and triplets). On the other hand, the $t_2^{DBH}$ state is a delocalized *p-d* hybrid, carrying both the vacancy dangling-bond characteristics and the distinct signature of the central atom, reflected by a node in the corresponding wave function at a distance shorter than half a bond length. The optical, magnetic, and electric characteristics of the system are decided by these orbitals, not by $e^{CFR}$ and $t^{CFR}$ valence-band states.

(iii) Concomitant with the delocalization of the gap orbitals, they are predicted to have only a small exchange splitting and multiplet separation. This is not sufficient to suppress Jahn-Teller distortions. Such distortions would then lower the symmetry of the gap orbital $t_2^{DBH}$, resulting in $a_+^1 a_-^1 b_+^1$-type level arrangement for the neutral centers, hence, with spin $S=\frac{1}{2}$. Electrical activity results from ionizations of these levels. Comparison of calculated and observed results suggests that, upon such ionizations, a relaxation energy of about 0.15—0.25 eV is involved for all charge states alike. This leads to Coulomb repulsion energies of $U \sim 0.3$ eV, representing the donor-acceptor splitting.

(iv) Only the neutral center is expected to be paramagnetic; the $A^+$ and $A^-$ centers are predicted both to have spin $S=0$. EPR of the neutral center would be observed if (a) complexes did not mask it; (b) the Fermi energy were between $E_v+0.35$ and $E_v+0.62$ eV, i.e., above the donor and below the acceptor level. In addition, a weak central hyperfine coupling constant will produce a small isotropic signal, split by the nuclear spin $I=\frac{3}{2}$ into four components, each being further split by the number of equivalent conformational structures of the relaxed defect. These factors contribute to the difficulty in observing the EPR of isolated gold impurity. Sample orientations may be needed to isolate a few of those lines.

(v) The charge distribution in the system indicates a partial depletion of the atomic *s* and *d* states and participation of the metal *p* states in bonding. Whereas Cu has all of its 11 valence electrons in the central cell, Ag and Au have lost about $0.5e$ through delocalization (not charge transfer). The effective impurity occupations are

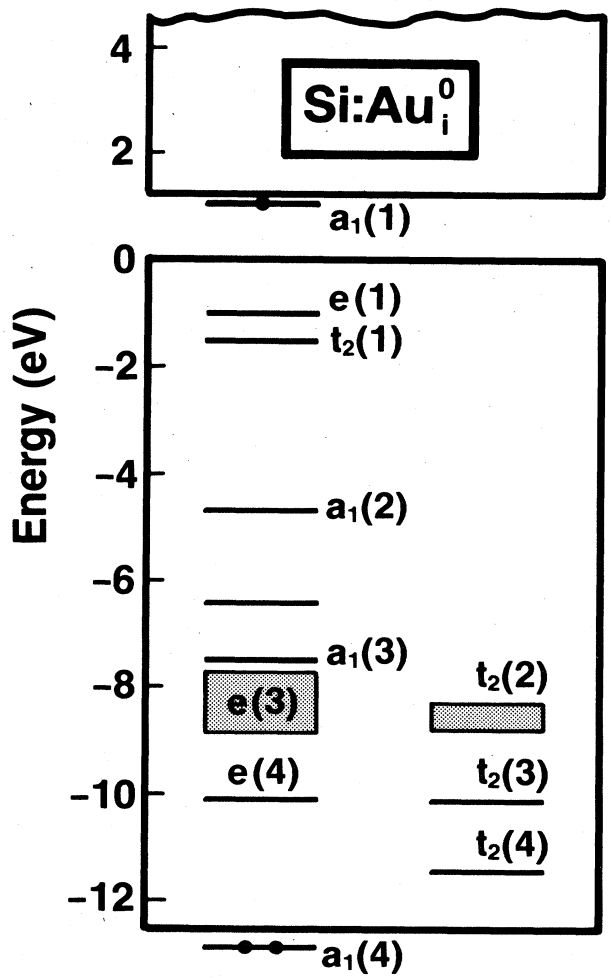


FIG. 8. Energy-level scheme resulting from a self-consistent (QBCF) calculation for the neutral gold interstitial in Si. Wave functions are depicted in Figs. 9—11.

Cu $s^{0.19}p^{0.84}(dfg)^{9.95}$, Ag $s^{0.22}p^{0.59}(dfg)^{9.68}$, and Au $s^{0.30}p^{0.65}(dfg)^{9.54}$.

## VI. INTERSTITIAL GOLD IN SILICON

We have calculated self-consistently the electronic structure of unrelaxed interstitial Au in the tetrahedral site of silicon. The energy levels obtained (Fig. 8) are profoundly different from those characterizing substitutional gold (cf. Fig. 3). We next discuss the various impurity-induced levels.

### A. $a_1$-like levels

We have found four impurity-induced $a_1$ resonances, denoted $a_1(1)$ through $a_1(4)$. In the gap, we find the very shallow $a_1(1)$ state, occupied by a single electron [i.e., $a_1^1(1)$] in the ground state of the neutral impurity $Si:Au_i^0$ (hence, an $S=\frac{1}{2}$ EPR signal might be observed, if sufficient interstitial concentration can be achieved, and no JT distortion is expected). Its wave function (Fig. 9) is quite delocalized (only $0.11e$ are enclosed in it within a nearest-neighbor sphere) and shows an antibonding node inside the central cell. This state can almost be characterized as an effective-mass-like donor state, bound by its screened Coulomb tail, with a small central-cell correction. A self-consistent calculation for the configuration $a_1^{0.5}(1)$ shows that the energy of the $a_1(1)$ state depends only weakly on its occupation, with $U_{ver}\simeq 0.025$ eV. The calculated donor transition energy is $\Delta E_{ver}^{1,0}\simeq\Delta E(0/+) < E_c - 0.1$ eV. This is the only electrically active level for the unrelaxed interstitial. Such an electrically active shallow donor has been observed[25(a)] in $Si:Cu_i$, which diffuses at 1100 °C in the $Cu^+$ charge state,[22(b)] but no reports for such a state in Si:Au (presumably, because of a combination of its low interstitial solubility and the difficulty in observing by DLTS a very shallow level) exist to our knowledge. Because of its delocalization, we expect the relaxation effect on this level to be rather small. Optical transitions to $a_1(1)$ from the VB may be observed as a structure near threshold. The deepest $a_1$ resonance [$a_1(4)$ in Fig. 9] is a bonding $s$-like state that appears slightly *below* the valence-band minimum. This localized state encompasses 36% of its charge in the central cell and constitutes the "fingerprint" of the interstitial impurity. We interpret the changes observed in the photoemission of Au-diffused silicon around the bottom of the valence band[15,20,21] as being associated with this $a_1(4)$ state. Between the $a_1(1)$ and $a_1(4)$ states we find the two additional $s$-like resonances $a_1(2)$ and $a_1(3)$ (another bonding-antibonding pair; cf. Fig. 9). We expect that the impurity-induced $a_1$ resonances $a_1(1)$ to $a_1(4)$ of $Si:Au_i$ will have a significant effect on the contact spin density.

It is interesting to compare the $s$-like, impurity-induced $a_1$ states obtained here with those predicted by a tight-binding model for interstitial $sp$-electron impurities in silicon.[95] This model predicts only two impurity-induced $a_1$ states below the conduction band: a bonding $a_1(4)$-like state and a nonbonding $a_1(1)$-like state in the upper part of the band gap (or just inside the conduction-band minimum). No $a_1(2)$ and $a_1(3)$ resonances are obtained in the simple tight-binding model; in addition, the $a_1(4)$-like states for all interstitials are predicted to be inside the upper part of the valence band, not below the valence-band minimum.

Our calculation for the $a_1$ resonances in $Si:Au_i$ suggests that it behaves qualitatively like monovalent group-IA interstitials in Si (Li,Na,K) in exhibiting only a simple shallow donor behavior. The only significant difference is that because of the far higher electronegativity of group-

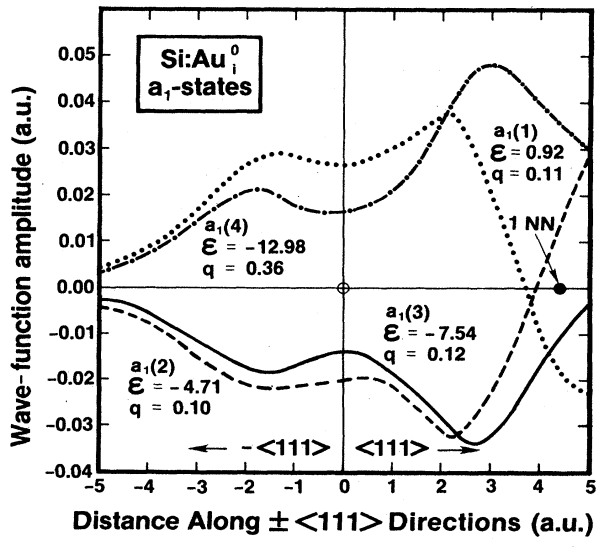


FIG. 9. Wave functions of impurity-induced $a_1$-type states of neutral interstitial gold in Si. The localization parameter $q$ denotes the total $(s+f)$ charge enclosed in a nearest-neighbor sphere for each state.

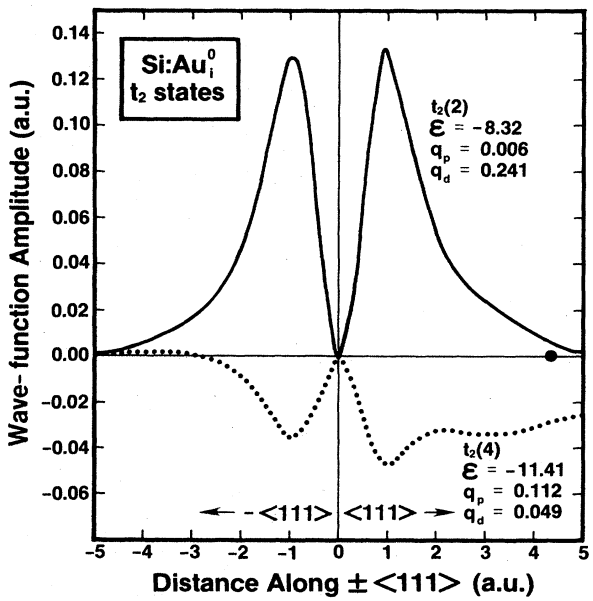


FIG. 10. Wave functions of impurity-induced $t_2$-type states of neutral interstitial gold in Si. The orbital localization parameters $q_p$ and $q_d$ denote the amount of $p$ and $d$ charge, respectively, enclosed for each state in a nearest-neighbor sphere.

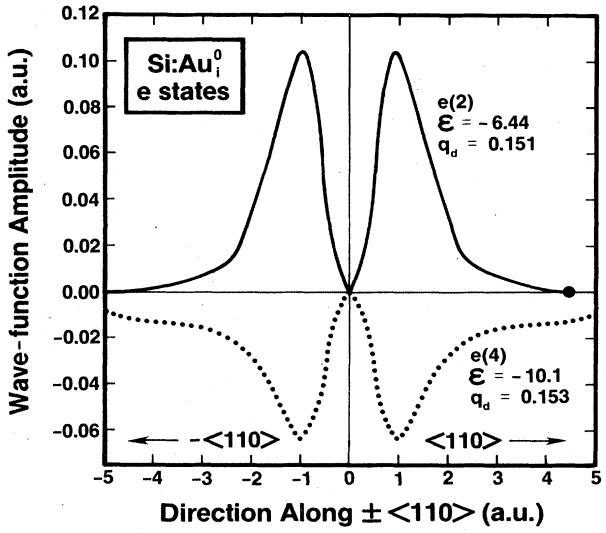


FIG. 11. Wave functions of impurity-induced $e$-type states of neutral interstitial gold in Si. The orbital localization parameter $q_d$ denotes the amount of $d$ charge enclosed for each state in a nearest-neighbor sphere.

I$B$ impurities (i.e., tighter valence $s$ electrons) relative to group-I$A$ impurities, the hyperdeep $a_1(4)$ state of the former is impuritylike and very deep, whereas in group-I$A$ interstitials the "hyperdeep" states are expected to be hostlike, located inside the valence band. A recent spin-polarized calculation[78(b),96] for Si:Cu$_i$ similarly shows a hyperdeep $a_1(4)$ state below the valence-band minimum, two hostlike resonances $a_1(3)$ and $a_1(2)$, and a virtual bound state of $a_1(1)$ type just at the conduction-band minimum. Upon ionization, this state moves down in energy, becoming weakly bound by the long-range Coulomb tail.

### B. $e$ and $t_2$-like levels

In contrast to the tetrahedral ordering of the $e$-$t_2$ levels in substitutional gold ($t_2^{\mathrm{DBH}}$ above $e^{\mathrm{CFR}}$), we find a reversed, octahedral ordering for the upper $e$ and $t_2$ levels in the interstitial system [$t_2(1)$ below $e(1)$ in Fig. 8]. The $t_2$ resonances appear again in bonding-antibonding pairs [$t_2(1)$ through $t_2(4)$ in Fig. 8] where the deepest state, $t_2(4)$, is predominantly a $p$ state (70%) with a smaller $d$ contribution. Its counterpart, $t_2(2)$, is more localized and is essentially a pure $d$ state (Fig. 10). Two examples of the deep $e$ resonances are given in Fig. 11. The charge distribution of all occupied states indicates Si:Au$_i^+$ (i.e., empty gap levels) behaves essentially as a free gold cation (i.e., $5d^{10}$-like). The $a_1(1)$ gap level in Si:Au$_i$ is higher in energy than the corresponding level of $sp$-electron interstitials (e.g., Al) because of the electron-electron repulsion from the $d$-like resonances in group-I$B$ impurities.

We interpret the fast diffusivity of positively charged interstitial gold (relative to, e.g., substitutional group-I$B$ impurities) to be a consequence of this extreme compactness of the $d^{10}$, Au$_i^+$ species and its very weak bonding to the lattice. We suspect that gold does diffuse mostly as a charged species: the failure to observe a field effect in the old drift experiments[23(b)] may be associated with the presence of gold-related complexes and the occurrence of only a small concentration of isolated interstitial Au$^+$. (Notice that only a small steady-state concentration of Si:Au$_i^+$ is needed to explain diffusion by an interstitial mechanism, whereas larger concentrations may be required to identify its electrical activity.) Furthermore, the stability of the closed-shell $\sim d^{10}$ structure of Si:Au$_i^+$ suggests that Si:Au$_i^{2+}$ is difficult to produce (as it requires the splitting of the stable $d^{10}$ shell); hence, no double-donor action is expected. For the perfect tetrahedral interstitial site, no deep acceptor action is expected either, as the $a_1^2(1)$ level is resonant just at the conduction-band minimum. However, an unoccupied $t_2$ resonance above the conduction-band minimum (very weak, and hence not shown in Fig. 8) could conceivably drop down into the band gap if the interstitial impurity moved away from its tetrahedral site. In this case, some acceptor action could be expected. Since the acceptor level of such an off-tetrahedral interstitial is lower in the gap than the acceptor level of the tetrahedral interstitial, its existence would lower the energy barrier for interstitial migration, leading to the possibility[97] of carrier-enhanced migration and solubility.

## VII. SUBSTITUTIONAL-INTERSTITIAL SITE EXCHANGE

Our study of the electrical levels of substitutional and interstitial gold in silicon suggests a simple energy-level scheme for the site exchange reaction, i.e., vacancy + interstitial → substitutional (Fig. 12). (We do not imply that the vacancy mechanism for diffusion is more important than the kick-out mechanism; we merely compare the level structure of substitutional and interstitial gold impurities, using the vacancy as a mediating link between the two.)

The various $t^n$-gap levels of the vacancy undergo lattice relaxation to produce the $\Delta E(0/+)$, $\Delta E(+/2+)$, $\Delta E(0/-)$, and $\Delta E(-/2-)$ electrical levels depicted in Fig. 12(a). The interstitial behaves as a simple single donor [Fig. 12(b)] with its $E(0/+)$ level near (or just at) the conduction-band minimum. When an interstitial is trapped in a vacancy site, it produces the (distorted) substitutional gold with levels depicted in Fig. 12(c). Its valence-band resonances are related generically to those of the interstitial system as illustrated by arrows in Fig. 12. The levels that remain in the gap are related generically to the vacancy levels. The level ordering is typical of a positive-$U$ system, except that when the substitutional and interstitial impurities are considered simultaneously, one finds the substitutional acceptor to be lower in the gap than the interstitial donor, a typical "negative-$U$" ordering.

It is interesting to compare the electrical levels of substitutional Si:Au to those of the silicon vacancy.[74] Denoting by $N$ the number of electrons in the gap levels, we have the $N=0$ systems $V^{2+}$ and Au$^{3+}$, the $N=1$ systems $V^+$ and Au$^{2+}$, the $N=2$ systems $V^0$ and Au$^+$, the $N=3$ systems $V^-$ and Au$^0$, and finally, the $N=4$ systems $V^{2-}$

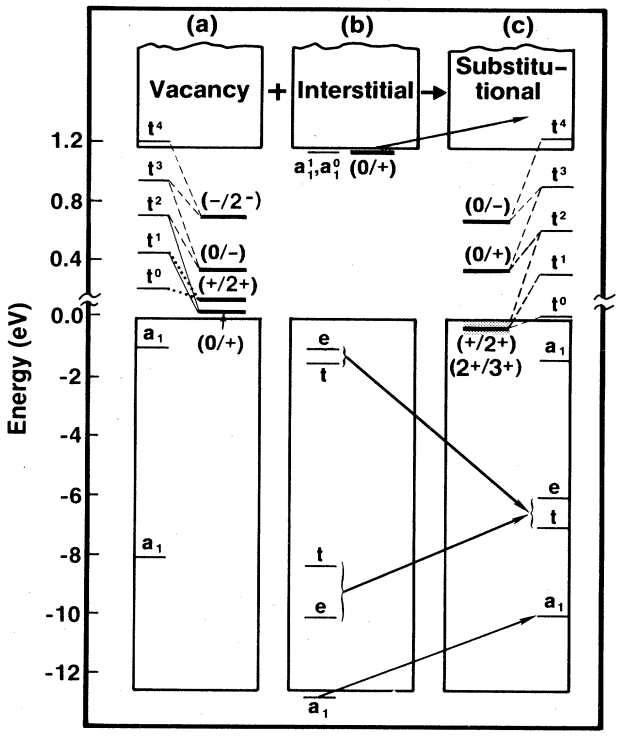


FIG. 12. Correspondence between the one-electron energy levels $t$, $e$, and $a_1$ (light horizontal lines) and electrical levels $(-/2-)$, $(0/-)$, $(0/+)$, $(+/2+)$, and $(2+/3+)$ (thick horizontal lines) of (a) the Si vacancy (data from Fig. 7 in Ref. 74), (b) Si:Au$_i$, and (c) Si:Au$_s$. The one-electron energy levels depend on their occupation number $N$ through Coulomb repulsion $U_{\rm ver}$. The electrical levels $(q/q')$ correspond to the change in total energy when a center with $N$ electrons in its gap level and charge state $A^q(N)$ is transformed into the center $A^{q'}(N')$ with a different number $(N')$ of electrons in its gap level and, hence, a different charge state $(q')$ as well. The dashed lines show the correspondence between a pair of one-electron levels (e.g., $t^4$ and $t^3$) and its associated electrical level [e.g., $(-/2-)$ for the vacancy, $(0/-)$ for Si:Au$_s$]. We have used $U_{\rm ver}=0.25$ eV for the vacancy (Ref. 74), $U_{\rm ver}=0.3$ eV for Si:Au$_s$, and $U_{\rm ver}=0.025$ eV for Si:Au$_i$, the last two are calculated here. The first and second acceptor levels of the vacancy are Watkins's guesses for experimental results [Fig. 7(c), Ref. 74]. The figure illustrates how the one-electron levels and the electrical levels of Si:Au$_s$ can be formed in the reaction vacancy $+$Si:Au$_i \leftrightarrows$Si:Au$_s$.

and $Au^-$. The $N=2,3,4$ system can show an $N=2\leftrightarrow N=3$ transition [first acceptor, $\Delta E^{2,3}(0/-)$ in the vacancy or first donor, $\Delta E^{2,3}(+/0)$ in Si:Au] as well as an $N=3\leftrightarrow N=4$ transition [double acceptor $\Delta E^{3,4}(-/2-)$ in the vacancy, first acceptor $\Delta E^{3,4}(0/-)$ in Si:Au]. For Si:Au we find the order of these levels to be normal, i.e., the donor $\Delta E^{2,3}(+/0)$ is lower in the gap than the acceptor $\Delta E^{3,4}(0/-)$. For the vacancy case, the information on the corresponding transitions $\Delta E^{2,3}(0/-)$ and $\Delta E^{3,4}(-/2-)$ is incomplete, but $V^-$ is known to exist, and the need to shine light on $n$-type silicon to produce $V^-$ was interpreted in terms of the existence of $V^{2-}$ (an EPR-invisible species) in this material. If an analogy is drawn with the corresponding states of gold, one would expect for the Si vacancy that $\Delta E^{2,3}(0/-)\simeq E_v+0.35$ eV and $\Delta E^{3,4}(-/2-)\simeq E_v+0.63$ eV. Experimental detection of the first and second acceptor levels in the Si vacancy could shed light on the correspondence to the first-donor and first-acceptor transition in Si:Au. The $N=0,1,2$ system can show an $N=0\leftrightarrow N=1$ transition [double donor $\Delta E^{0,1}(2+/+)$ for the vacancy, triple donor $\Delta E^{0,1}(3+/2+)$ for Si:Au], and an $N=1\leftrightarrow N=2$ transition [single donor $\Delta E^{1,2}(+/0)$ for the vacancy, double donor $\Delta E^{1,2}(2+/+)$ or Si:Au]. For the Si vacancy, the order of these transitions corresponds to an "Anderson negative-$U$" situation,[74] i.e., the single donor (at $E_v+0.05$ eV) is lower in the gap than the double donor (at $E_v+0.13$ eV). Analogy with Si:Au would suggest the double donor to be lower in energy than the triple donor; however, both of these states in Si:Au are likely to reside just below the valence-band maximum. This situation is depicted in Fig. 12.

The reasons that the Si:Au $N=2,3,4$ system might exhibit a positive-$U$ behavior relative to the $N=0,1,2$ vacancy system are (i) $U_{\rm ver}$ for Si:Au is somewhat larger than the corresponding value for the vacancy due to the existence of a small $d$-orbital component in the former case, and (ii) the elastic force-constant $K$ coupling the defect to the lattice is larger for Si:Au (where some bonds with nearest-neighbor ligands are formed through the $t_2^{\rm CFR}$ states) than for the Si vacancy (which lacks $t^{\rm CFR}$). Since the relaxation correction $\Delta U_R$ (cf. Sec. V D) is inversely proportional to $K$, a smaller JT energy may be associated with Si:Au. Finally, note that even in the vacancy system, the linear JT coupling constant for the $N=2,3,4$ system is smaller than in the $N=0,1,2$ system, which suggests a weaker JT energy in the former case.

It is interesting to contrast this energy-level scheme with the one recently proposed by Bagraev and Mashkov[98] to explain the extremely slow recombination tunneling rates[99] in Si:Au. They proposed negative-$U$ ordering of the levels of substitutional gold [the $E(0/-)$ acceptor at $E_v+0.68$ eV below the substitutional donor whose position remains unspecified in their model], but a normal-level ordering for interstitial gold [the $E(0/+)$ donor at $\sim E_v+0.35$ eV, below the interstitial acceptor whose position is also unspecified]. Hence, at the substitutional site the lowest-energy species is $Au_s^-$ (below $Au_s^+$ and $Au_s^0$, the latter being metastable), whereas at the interstitial site, the lowest-energy species is $Au_i^0$ (below $Au_i^+$ and $Au_i^-$). The reason that $Au_i^0$ (and not $Au_i^+$) is the lowest-energy species at the interstitial site is argued to be a new version of the Anderson negative-$U$ effect,[100] where the electron-phonon coupling constant for the substitutional-to-interstitial jump is set to be zero for $Au_i^+$ and $Au_i^-$ but taken to be nonzero for $Au_i^0$. While no justification is given for the appropriateness of these assumptions for Si:Au, the model does have the appealing feature of explaining the very slow $Au_i^0+e\rightarrow Au_s^-$ reaction in terms of an *activated transition* between the ground state of the interstitial center $Au_i^0$, to the ground state of the substitutional center $Au_s^-$. However, other interpretations are also possible.[99] Our calculation is consistent with the ob-

served electrical levels, if a simple, positive-$U$-like ordering is assumed for the distorted substitutional site, and the present calculation does not support the hypothesis[98] of a deep donor (at $E_v+0.35$ eV) at the interstitial site. Instead, we find a very shallow donor at (or above) $E_c-0.1$ eV. Reexamination of their[98] experiment on the paramagnetic center after prolonged optical pumping is needed.

The relative level arrangement for substitutional and interstitial gold in Si suggests a simple mechanism for[25] relative substitutional versus interstitial solubilities and its doping dependence: a smaller enthalpy of solution (hence larger solubility) is expected at the substitutional site due to its deeper electrical levels. Other factors distinguishing substitutional from interstitial binding energies to the lattice include the different nature of their bonding states (compare Fig. 3 with Fig. 8). The relative substitutional solubilities of different group-I$B$ impurities (or in different host crystals) is related, in turn, to the variations in the positions and widths of the bonding $t_2^{\mathrm{CFR}}$ states that are responsible for bond formation with the lattice.

## ACKNOWLEDGMENT

The authors are grateful to J. Corbett, M. Höhne, L. Å. Ledebo, and E. Weber for their useful comments on the manuscript. M.J.C. and A.F. acknowledge support from FAPESP, Brasil.

*Present address: Institute of Physics, University of São Paulo, São Paulo, Brazil.

†Present address: Instituto de Fisica, Univérsidade Estadual de Campinas (UNICAMP), Campinas, São Paulo, Brazil.

[1]A. Zunger, Ann. Rev. Mater. Sci. (to be published).

[2]L. A. Hemstreet, in *Thirteenth International Conference on Defects in Semiconductors,* edited by L. C. Kimerling and J. M. Parsey (The Metallurgical Society, Warrendale, 1985), p. 1043.

[3]G. D. Watkins, G. G. DeLeo, and W. B. Fowler, Physica **116B**, 28 (1983).

[4]B. G. Cartling, J. Phys. C **8**, 3183 (1975).

[5]A. Fazzio and J. R. Leite, Phys. Rev. B **21**, 4710 (1980).

[6]P. Pecheur and G. Toussaint, Physica **116B**, 112 (1983).

[7]H. Katayama-Yoshida and K. Shindo, Solid State Commun. **44**, 989 (1982).

[8]U. Lindefelt and A. Zunger, Phys. Rev. B **30**, 1102 (1984).

[9]*Landolt-Börnstein Numerical Data and Functional Relationships in Science and Technology,* edited by O. Madelung (Springer, Berlin, 1982), Vols. 17a and 17b.

[10](a) S. Sugano, Y. Tanabe, and H. Kamimura, *Multiplets of Transition Metal Ions in Crystals* (Academic, New York, 1970); (b) J. E. Huheey, *Inorganic Chemistry,* 3rd ed. (Harper and Row, New York, 1983), p. 359.

[11]J. W. Chen and A. G. Milnes, Ann. Rev. Mater. Sci. **10**, 157 (1980); A. G. Milnes, *Deep Impurities in Semiconductors* (Wiley-Interscience, New York, 1973).

[12]M. L. Joshi and S. Dash, J. Appl. Phys. **37**, 2453 (1966).

[13]R. H. Wu and A. R. Peaker, Solid State Electron. **25**, 643 (1982); H. Lemke, Phys. Status Solidi A **75**, 473 (1983).

[14]J. R. Davis, A. Rohatgi, R. H. Hopkins, R. D. Blais, P. Rai-Choudhury, J. McCormick, and H. C. Mollenkopf, IEEE Trans. Electron Devices **ED-27**, 677 (1980).

[15]L. Braicovich, C. M. Ganner, P. R. Sleath, C. Y. Su, P. W. Chye, I. Lindau, and W. E. Spicer, Phys. Rev. B **20**, 5131 (1979).

[16]A. Franciosi, D. G. O'Neill, and J. H. Weaver, J. Vac. Sci. Technol. B **1**, 524 (1983).

[17]A. Hiraki, M. A. Nicolet, and J. W. Mayer, Appl. Phys. Lett. **18**, 178 (1971); T. Narusawa, S. Komiya, and A. Hiraki, *ibid.* **22**, 389 (1973); A. Hiraki, K. Shuto, S. Kim, W. Kammura, and M. Iwami, *ibid.* **31**, 611 (1977).

[18]A. K. Green and E. Bauer, J. Appl. Phys. **47**, 1284 (1976).

[19]I. Abbati, L. Braicovich, and A. Franciosi, Solid State Commun. **33**, 881 (1980); I. Abbati, L. Braicovich, A. Franciosi, I. Lindau, P. R. Skeath, C. Y. Su, and W. E. Spicer, J. Vac. Sci. Technol. **17**, 930 (1980).

[20]A. McKinley, R. H. Williams, and A. W. Parke, J. Phys. C **12**, 2447 (1979).

[21]G. Rossi, I. Abbati, L. Braicovich, I. Lindau, and W. E. Spicer, Surf. Sci. **112**, L765 (1981).

[22](a) W. R. Wilcox and T. J. LaChapelle, J. Appl. Phys. **35**, 240 (1964); (b) N. A. Stolwijk, B. Schuster, J. Hölzl, H. Mehrer, and W. Frank, Physica **116B**, 335 (1983); (c) M. Morooka, H. Tomokage, H. Kitagawa, and M. Yoshida, Jpn. J. Appl. Phys. **24**, 133 (1985).

[23]C. J. Gallagher, J. Phys. Chem. Solids **3**, 82 (1957).

[24]J. A. Van Vechten and C. D. Thurmond, Phys. Rev. B **14**, 3539 (1976).

[25](a) R. N. Hall and J. H. Racette, J. Appl. Phys. **35**, 379 (1964); (b) S. L. Chou and J. F. Gibbons, *ibid.* **46**, 1197 (1975).

[26]B. I. Boltaks and H. Shih-Yin, Fiz. Tverd. Tela **2**, 2677 (1960). [Sov. Phys.—Solid State **2**, 2383 (1961)].

[27]F. A. Trumbore, Bell Syst. Tech. J. **39**, 205 (1960).

[28]V. A. Singh and A. Zunger, Phys. Rev. B **25**, 907 (1982).

[29](a) Y. H. Lee, R. L. Kleinhenz, and J. W. Corbett, in *Defects and Radiation Effects in Semiconductors, 1978* edited by J. H. Albany (The Institute of Physics, Bristol, 1979), Vol. 46; (b) R. L. Kleinhenz, Y. H. Lee, J. W. Corbett, E. G. Sieverts, S. H. Muller, and C. A. J. Ammerlaan, Phys. Status Solidi B **108**, 363 (1981).

[30](a) J. Utzig and W. Schröter, Appl. Phys. Lett. **45**, 761 (1984); (b) S. D. Brotherton, P. Bradley, A. Gill, and E. R. Weber, J. Appl. Phys. **55**, 952 (1984).

[31]L. C. Kimerling, J. L. Benton, and J. J. Rubin, in *Proceedings of the 11th Conference on Defects and Radiation Effects in Semiconductors, Oiso, Japan, 1980,* edited by R. R. Hasiguti (IOP, London, 1981).

[32]K. Graff and H. Pieper, J. Electrochem Soc. **128**, 669 (1981); R. Gleichmann, H. Blumtritt, and J. Heydenreich, Phys. Status Solidi A **78**, 527 (1983).

[33]A. A. Lebedev and A. T. Mamadalimov, Fiz. Tekh. Poluprovodn. **6**, 2409 (1972); A. A. Lebedev, A. T. Mamadalimov, and Sh. Makhkamoi, **6**, 2918 (1972) [Sov. Phys.—Semicond. **6**, 2019 (1973); **6**, 1853 (1973)].

[34]P. C. Smith and A. G. Milnes, Int. J. Electron. **30**, 225 (1971); **32**, 697 (1972).

[35]F. L. Thiel and S. K. Ghandhi, J. Appl. Phys. **41**, 254 (1970).

[36]A. J. Tavendale and S. J. Pearton, J. Phys. C **16**, 1665 (1983); **17**, 6701 (1984).

[37]S. D. Brotherton and J. Bicknell, J. Appl. Phys. **49**, 667 (1978).
[38]S. Braun and H. G. Grimmeiss, J. Appl. Phys. **45**, 2658 (1974).
[39]K. D. Glinchuk and N. M. Litovchenko, Fiz. Tverd. Tela **6**, 3701 (1964) [Sov. Phys.—Solid State **6**, 2963 (1965)].
[40]D. V. Lang, H. G. Grimmeiss, E. Meijer, and M. Jaros, Phys. Rev. B **22**, 3917 (1980).
[41](a) C. T. Sah, L. Forbes, L. I. Rosier, A. F. Tasch, and A. B. Tole, Appl. Phys. Lett. **15**, 145 (1969); (b) L. D. Yau and C. T. Sah, *ibid.* **21**, 157 (1972).
[42]O. Engström and H. G. Grimmeiss, J. Appl. Phys. **46**, 831 (1975).
[43]W. Fahrner and A. Goetzberger, Appl. Phys. Lett. **21**, 329 (1972).
[44]K. D. Glinchuk, A. D. Denisova, and N. M. Litovchenko, Fiz. Tverd. Tela **7**, 3669 (1966) [Sov. Phys.—Solid State **7**, 2963 (1966)].
[45]J. Mazzaschi, J. C. Brabant, Mme. B. Brousseau, J. Barrau, M. Brousseau, F. Voillot, and P. Bacuvier, Solid State Commun. **39**, 1091 (1981).
[46]L. Å. Ledebo and Zhan-Guo Wang, Appl. Phys. Lett. **42**, 680 (1983).
[47]R. M. Feenstra and S. T. Pantelides, Phys. Rev. B (to be published).
[48]K. Nagasawa and M. Schulz, Appl. Phys. **8**, 35 (1975).
[49](a) J. E. Lowther, J. Phys. C **13**, 3665, 3681 (1980); (b) S. D. Brotherton and J. E. Lowther, Phys. Rev. Lett. **44**, 606 (1980).
[50]R. Kassing, L. Cohausz, P. van Staa, W. Mackert, and H. J. Hoffman, Appl. Phys. A **34**, 41 (1984).
[51]B. Brückner, Phys. Status Solidi A **4**, 685 (1975).
[52]H. I. Ralph, J. Appl. Phys. **49**, 672 (1978).
[53]M. Höhne, Phys. Status Solidi B **99**, 651 (1980); **109**, 525 (1982); **119**, K117 (1983).
[54]V. S. Postnikov, V. I. Kirillov, Yu. A. Kasputin, N. N. Pribylov, Yu. I. Kozlov, and V. V. Misneev, Fiz. Tekh. Poluprovodn. **14**, 2265 (1980) [Sov. Phys.—Semicond. **14**, 1342 (1980)].
[55]G. D. Watkins, in *Lattice Defects in Semiconductors 1974* (IOP, London, 1975), p. 1.
[56]G. W. Ludwig and H. H. Woodbury, Phys. Rev. **126**, 466 (1962).
[57](a) J. C. M. Henning and E. C. J. Hgelmeers, Phys. Rev. B **27**, 4002 (1983); (b) R. F. Milligan, F. G. Anderson, and G. D. Watkins, *ibid.* **29**, 2819 (1984).
[58]D. Thebault, J. Barrau, M. Bousseau, Do Xuan Thanh, J. C. Brabant, F. Voillot, and M. Ribault, Solid State Commun. **45**, 645 (1983).
[59]G. W. Ludwig and H. H. Woodbury, in *Solid State Physics,* edited by F. Seitz and D. Turnbull (Academic, New York, 1962), Vol. 13, p. 223.
[60]U. Kaufmann and J. Schneider, Adv. Electron. Electron Phys. **58**, 81 (1983).
[61]W. Low and E. L. Offenbacker, in *Solid State Physics,* edited by F. Seitz and D. Turnbull (Academic, New York, 1965), Vol. 17, p. 135.
[62]C. J. Ballhausen, *Ligand Field Theory* (McGraw-Hill, New York, 1962).
[63]J. B. Goodenough, *Magnetism and the Chemical Bond* (Wiley, New York, 1963).
[64]B. H. Brandow, Adv. Phys. **26**, 651 (1977).
[65]A. Zunger and M. L. Cohen, Phys. Rev. B **20**, 1189 (1979).
[66]A. Fazzio and A. Zunger, Solid State Commun. **52**, 265 (1984).
[67]A. Fazzio, M. J. Caldas, and A. Zunger, Phys. Rev. B **30**, 3430 (1984).
[68]C. Pedrini and H. Chermette, Int. J. Quantum Chem. **23**, 1025 (1983).
[69]H. Chermette and C. Pedrini, J. Chem. Phys. **75**, 1869 (1981).
[70]J. G. Harrison and C. C. Lin, Phys. Rev. B **23**, 3894 (1981).
[71]D. D. Chase and D. S. McClude, J. Chem. Phys. **64**, 74 (1976).
[72]L. H. Ahrens, *Ionization Potentials* (Pergamon, Oxford, 1983).
[73]A. Zunger and U. Lindefelt, Phys. Rev. B **27**, 1191 (1983).
[74]G. D. Watkins, Physica **117&118B**, 9 (1983).
[75]F. A. Cotton and G. Wilkinson, *Advanced Inorganic Chemistry* (Wiley, New York, 1972).
[76]T. Hoshino and K. Suzuki, J. Phys. Soc. Jpn. **48**, 2031 (1980).
[77]A. Zunger and U. Lindefelt, Phys. Rev. B **26**, 5989 (1982); U. Lindefelt and A. Zunger, J. Phys. C **17**, 6047 (1984).
[78](a) H. Katayama-Yoshida and A. Zunger, Phys. Rev. Lett. **53**, 1256 (1984); (b) Phys. Rev. B **31**, 8317 (1985).
[79]L. S. Kogan and K. B. Tolpygo, Fiz. Tverd. Tela **15**, 1544 (1973); **16**, 3176 (1974) [Sov. Phys.—Solid State **15**, 1034 (1973); **16**, 2067 (1975)].
[80]J. L. A. Alves, J. R. Leite, L. V. C. Assali, V. M. S. Gomes, and C. E. T. Goncalves da Silva, J. Phys. C **17**, L771 (1984); J. L. A. Alves and J. R. Leite, Phys. Rev. B **30**, 7284 (1984).
[81]This effect is not seen for strongly hybridized states, A. Dal Pino, A. Fazzio, and J. R. Leite, Solid State Commun. **44**, 369 (1982); A. Dal Pino and A. Fazzio, Rev. Bras. Fis. (Semiconductors) Special Issue, 436 (1983).
[82](a) L. A. Hemstreet, Phys. Rev. B **22**, 4590 (1980); (b) A. Fazzio and J. R. Leite, *ibid.* **21**, 4710 (1980).
[83]C. E. Moore, *Atomic Energy Levels,* Nat. Stand. Ref. Data. Ser. Nat. Bur. Stand. Pub. No. 35 (U.S. GPO, Washington, D.C., 1971).
[84]C. Froese Fisher, *The Hartree-Fock Method for Atoms* (Wiley-Interscience, New York, 1977).
[85]J. C. Slater, *Symmetry and Energy Bands in Crystals* (Dover, New York, 1972), p. 55.
[86]U. Lindefelt and A. Zunger, Phys. Rev. B **24**, 5913 (1981); **26**, 846 (1982).
[87]A. Zunger, Phys. Rev. B **22**, 649 (1980).
[88]L. Kleinman, Phys. Rev. B **21**, 2630 (1980).
[89]A. Zunger and M. L. Cohen, Phys. Rev. B **18**, 5449 (1978); **20**, 4082 (1979).
[90](a) A. Zunger, Phys. Rev. Lett. **50**, 1215 (1983); (b) V. Singh and A. Zunger, Phys. Rev. B **31**, 3729 (1985).
[91]V. A. Singh, A. Zunger, and U. Lindefelt, Phys. Rev. B **27**, 1420 (1983); V. A. Singh, U. Lindefelt, and A. Zunger, *ibid.* **27**, 4909 (1983).
[92]A. Zunger and U. Lindefelt, Solid State Commun. **45**, 343 (1983).
[93]A. F. Wells, *Structural Inorganic Chemistry,* 4th ed. (Clarendon, Oxford, 1975), p. 875.
[94]R. D. Shannon, in *Structure and Bonding in Crystals,* edited by M. O'Keefe and A. Navrotsky (Academic, New York, 1981), Vol. II, p. 53.
[95]O. F. Sankey and J. D. Dow, Phys. Rev. B **27**, 7641 (1983).
[96]H. Katayama-Yoshida and A. Zunger (unpublished).
[97]G. A. Baraff and M. Schlüter, Phys. Rev. B **30**, 3460 (1984).
[98]N. T. Bagraev and V. A. Mashkov, Pis'ma Zh. Eksp. Teor. Fiz. **39**, 211 (1984) [JETP Lett. **39**, 251 (1984)]; Solid State Commun. **51**, 515 (1984).
[99]W. P. Brickley and D. V. Eddolls, Solid State Electron. **21**, 1616 (1978).
[100]P. W. Anderson, Phys. Rev. Lett. **34**, 953 (1975).